BIOCHEMICAL MODIFICATION of BIODEGRADABLE NANOFIBERS

by

Onur Arslan

B.S., Textile Engineering, Uşak University, 2008

B.S., Management, Anadolu University, 2011

Submitted to the Institute of Biomedical Engineering

in partial fulfillment of the requirements

for the degree of

Master of Science

in

Biomedical Engineering

Boğaziçi University

2014

ACKNOWLEDGMENTS

Apart from the efforts of myself, completion of this thesis depends on the encouragement and guidelines of many others. I take this opportunity to express my gratitude to the people who have been helpful during studies on my thesis.

First and foremost, I offer my sincerest gratitude to my advisor Asist. Prof. Dr. Bora Garipcan for his continuous support and the valuable guidance and advice. One simply could not wish for a better or friendlier supervisor. I would also like to thank to my committee members Prof. Dr. Murat Gülsoy and Assoc. Prof. Dr. Lokman Uzun for their valuable insight, contributions, suggestions and their existence in my thesis committee.

I would also like to thank to my Assoc. Prof. Dr. Kadriye Tuzlakoğlu and Assoc. Prof. Dr. Sevil Dinçer for their help and supports in my previous studies to enlighten my thesis.

I would like to thank Aykut Arif Topçu, Gülsu Şener for their help in FTIR, and contact angle characterizations.

I'm particularly grateful to Elif Dönmez for his assistance with the XPS graphs used in this thesis and to Dr. Çağrı Kaan Akkan for the suggestions in editing process. I would also like to thank my other colleague friends in my Biomaterial Laboratory for their support and motivation.

Lastly I would like to give special thanks to my family. I always have felt their good wishes during my thesis work. I wish to thank my parents Erdoğan Arslan, Gülfidan Arslan and my brother Gökhan Arslan for supporting me.

ABSTRACT

BIOCHEMICAL MODIFICATION of BIODEGRADABLE NANOFIBERS

Organ and tissue losses caused by a disease or a trauma can be treated by variety of sources such as; autograft, allograft and xenograft. Providing the cells from these sources have many disadvantages like; difficulty of finding a suitable donor, rejection of the tissue by the body and immune system related problems. In order to overcome those problems tissue engineers try to produce required tissue in the laboratories with few cells which are taken from the patient. In this context, in order to fabricate desired tissue cultures, many efforts are going on development of various cell scaffold materials, surfaces and biochemicals. Although our knowledge on this subject increases in time, more studies are needed to be done. In the purpose of this thesis, histidine and fetuin immobilized Poly-ϵ-caprolactone (PCL) membranes and nanofiber meshes were prepared to enhance biocompatibility. PCL nanofiber meshes were produced via electrospinning and PCL membranes by solvent casting method. For the surface modification in the first step, hexamethylenediamine (HMDA) was used to introduce amino groups onto the PCL surfaces. Histidine, and fetuin immobilization on amino groups of the surface carried out by using cyanamide and N-hydroxysuccinimide (NHS). Fourier Transform Infrared Spectroscopy (FTIR), X-ray Photoelectron Spectroscopy (XPS) and Scanning Electron Microscopy (SEM) were used for the characterization of modifications. The effects of surface modification on cell proliferation were studied by using L929 fibroblast-like cells. MTT assay and cell cultures studies have shown that histidine modified PCL nanofiber meshes have shown higher cell proliferation percentage than histidine modified PCL membranes and control groups within increasing histidine content. According to the results it was shown that PCL biocompatibility can be enhanced with such simple amino acid histidine and it is possible to use these surfaces in many different tissue engineering applications.

Keywords: Polycaprolactone, Nanofiber, Histidine, Fetuin, Electrospinning.

ÖZET

BİYOBOZUNUR NANOFİBERLERİN BİYOKİMYASAL MODİFİKASYONU

Hastalık veya travma sonucu meydana gelen organ ve doku kayıpları otograft, allograft ve zenograft gibi farklı kaynaklarla tedavi edilebilinmektedir. Bu kaynaklardan sağlanan hücrelerin, uygun bağışçı bulma, doku reddi ve bağışıklık sistemi ile ilgili problemler gibi bir çok dezavantajı vardır. Bu problemleri aşmak için doku mühendisleri gerekli dokuyu hastadan alınan az miktarda hücre ile laboratuvarda üretmeye çalışmaktadır. Bu bağlamda arzulanan doku kültürlerini oluşturabilmek için çeşitli hücre iskelesi malzemeleri, yüzeyleri ve biyokimyasallar üzerinde emek harcanmaktadır. Bu konudaki bilgimiz zamanla artsa da daha fazla çalışma yapılması gerekmektedir. Bu tezin amacı, hisitidin ve fetüin immobilize Poli-(ϵ)-kaprolakton (PCL) membran ve nanofiber örgüleri hazırlayarak PCL'nin biyouyumluluğunu geliştirmekdir. PCL nanofiber örgüler elektroeğirmeyle ve PCL membranlar ise çözelti dökme yöntemiyle üretilmiştir. Yüzeylerin modifikasyonu için önce heksametilendiamin (HMDA) kullanılarak PCL yüzeylerde amino grupları oluşturulmuştur. Yüzeydeki amino grupları üzerine histidin ve fetüin bağlanması siyanamid ve N-hidroksisüksinimid (NHS) yardımıyla gerçekleştirilmiştir. Fourier dönüşümlü kızılötesi spektroskopisi (FTIR), X-ray fotoelektron spektroskopisi (XPS) ve taramalı elektron mikroskobu (SEM), modifikasyonların karakterizasyonunda kullanılmıştır. Yüzey modifikasyonunun hücre üremesine etkileri, L929 fibroblast benzeri bağ doku hücreler kullanılarak incelenmiştir. Hücre kültürleri ve yapılan MTT testi ve hücre kültürü çalışmalarında, histidin miktarındaki artışla orantılı olarak, histidin modifiye PCL nanofiber örgüleri, histidin modifiyeli PCL membran ve diğer kontrol gruplarından daha yüksek hücre büyümesi yüzdesi göstermiştir. Sonuçlar PCL'nin biyouyumluluğunun basit bir amino asit ile geliştirilebildiğini ve bu yapıların bir çok farklı doku mühendisliği uygulamasında kullanılabileceğini göstermiştir.

Anahtar Sözcükler: Polikaprolakton, Nanolif, Histidin, Fetüin, Elektroeğirme.

TABLE OF CONTENTS

LIST OF FIGURES

LIST OF TABLES

LIST OF SYMBOLS

μm	Micrometer
°C	Degree of celsius

LIST OF ABBREVIATIONS

PCL	Poly-ϵ-caprolactone
DMF	Dimethylformamide
DNA	Deoxyribonucleic Acid
ECM	Extracellular Matrixl
PLA	Polylactic Acid
PGA	Polyglucolic Acid
NF	Nanofiber
PM	Plain Membrane
HMDA	Hexamethylenediamine
rpm	Revolutions Per Minute
TGF	Transforming Growth Factor
IPA	Isopropanol
SEM	Scanning Electron Microscopy
XPS	X-ray Photoelectron Spectroscopy
FTIR	Fourier Transform Infrared Spectroscopy
His	Histidine

1. INTRODUCTION

1.1 Motivation

Desire of the health sciences is prolonging the human life and increasing the quality. A healthy immortal life will be the last resort of this aim. In order to extend our lives we need to fabricate tissues and organs to replace existing worn-out part of the body.

A disease or an external physical effect can damage organs. Regeneration capacity is limited for many adult cells. Injures can be permanent. Clinical treatments mostly focus on minimizing further tissue loss and relieve symptoms by applying pharmaceuticals and rehabilitation techniques [1]. However, these practices have limited effects, with additional some side-effects as well [2]. In terms of surgery, there are different approaches for the reconstruction of organ or tissue. One of them is transplanting tissue from other parts of the body which is called autologous grafting. However, it has some drawbacks such as multiple surgical procedures and loss of function at the donor site. Transplanting from other human donor (allograft) or an animal (xenograft) is not a perfect solution either. These surgical operations may have immune response problems and finding a compatible donor for allograft is an other problem. When self healing is not an option, a biocompatible scaffold can provide a physical and chemical support for the cell growth and regeneration [3].

Controlling cell proliferation and differentiation is a must to produce needed tissues. Cells in our body need not just neighbor cells also extracellular matrix (ECM). Extracellular matrix (ECM) possess fibrils mostly, diameters between tens of nanometers to micrometers. ECM provides structural, biochemical support and also, a store for cell signaling chemicals. Thus, the structure of these matrix fibrils serves as guide in fabrication of tissue morphology. Tissue scaffolds are designed to be substitute for ECM and promote cell proliferation and differentiation as desired. One of the main

goal of tissue engineering is producing the perfect tissue scaffold, and many researchers in biomaterial science try to improve existed scaffolds and to find novel ones for various tissue types [4].

Materials such as biodegradable [5] and non-biodegradable [6, 7, 8] polymers have been investigated as potential scaffold materials. Considering the elimination of a second surgery, biodegradable polymers are preferred over others. Thus, biodegradable polymers should comprehensively evaluated regarding their biocompatibility and degradable behaviors. Nevertheless, improving the interactions between the biomaterials and the cells is still a big challenge.

There are many biodegradable polymers like, Polylactic acid (PLA) [9], Poly-ϵ-caprolactone (PCL) [10], polyglycolide (PGL) [11] and their copolymers used as scaffolds. Poly-ϵ-caprolactone is relatively cheap and easily accessible material which has approvals from Food and Drug Administration (FDA) in the USA and the Therapeutic Goods Administration in the Australia for implantation usages [12, 13]. It has a a significant long degradation time which can lasting up to 4 year [12, 14]. Therefore, it is popular on the long term implantlation applications [15]. The successful introduction of cell cultures in a porous PCL matrix has been reported [16, 17]. On the other hand PCL is not a perfect polymer, in terms of cytocompatibility. Thus, to enhance cytocompatibility, modification of PCL is necessary [18].

It is well known that surface properties of a scaffold play a crucial role in supporting cellular behaviors such as adhesion, proliferation, [19, 20]. It was expected that, PCL membranes and nanofiber meshes surfaces effect to the cells differently. As pointed out above PCL has approvals from globally recognized foundations. There are many PCL products related with scaffolds studies in the market such as; "12-well Multi-Well plates with 3D polycaprolactone Scaffolds (Life Science Products Inc.)", "Celltreat 3D Polycaprolactone (PCL) Cell Culture Plates (Globe Bio & 3D Biotek Llc)". However these scaffolds has averagely 300 μm diameter fibers and, an average human cell's size is roughly 10-20 micron [21]. Synthetic microfibers are similar in size to most cells, therefore, attached cells on microfibers can be considered in a 2D envi-

ronment with a curvature [22]. Cells prefer mostly nano size structures for adhesion due to the increased contact point [23]-[28]. Including to that, nanofibers possess large surface area, which allows more ligand immobilization on the surface of fibers resulted with increased number of contact points. Moreover, similarity between the natural extracellular matrix and the nanofiber scaffolds in terms of 3 D architecture also provide more closer environment to the desired one [29]. For this purpose electrospinning technique can be utilized to fabricate random and/or aligned nanofiber scaffolds with various sizes in diameter [4].

In this thesis, to increase the biocompatibility of PCL, histidine and fetuin biomolecules immobilized on PCL membranes and nanofiber meshes. Histidine and fetuin are chosen as having a functional side chain such as imidazole and fetuin a sialic acid containing laminin like adhesive protein, respectively. In order to observe effects of non-modified, histidine and fetuin modified Poly-ϵ-caprolactone (PCL) membranes and nanofibers on cell growth, fibroblasts cells (L929) were cultured on these surfaces.

1.2 Objectives

The fundamental aim is to fabricate biocompatible, biodegradable polymeric scaffolds with simple biochemical modifications. Objectives to support the aim of the thesis are as follow:

- To investigate the effects of 'histidine' amino acid and 'fetuin' protein immobilization on the biocompatibility of PCL membranes and nanofiber meshes,
- To investigate the effect of 'histidine' content on the biocompatibility of PCL membranes and nanofiber meshes,
- To investigate the effect of production methods of PCL surfaces with electrospining and casting methods on cell growth.

- To investigate the effects of histidine immobilization on in-vitro biodegradation of PCL nanofibers.

1.3 Outline

The thesis is presented at 5 chapters, In the second chapter, fundamental information about the biodegradable materials, Poly-ϵ-caprolactone, nanofibers, electrospining, histidine, and lastly fetuin were given. In chapter 3, materials and the experimental procedures were described. In chapter 4, the results were presented. In the last chapter, the discussion of the results and the possible implications were discussed.

2. BACKGROUND

2.1 Biodegradable Polymers

Polymers are large molecules consisting of small repeatable subunits so called monomers. Polymers can be divided into two subgroups which are natural and synthetic. Natural polymers, such as starch, cellulose, natural rubber, DNA, are existed in nature while synthetic polymers are derived from crude oil fractions. Synthetic polymers find places in our daily lives since the 1950s, and today, they are in every aspect of life with numerous applications, thanks to their low cost and diverse features. [30].

Together with metals, ceramics, composites and polymers can also be used for biological applications as materials which can interact with biological systems [31]. Although numerous polymers are available, very small portion of produced polymers are used as biomaterials. Most traditional synthetic polymers show high endurance and do not degradate for many years. On the other hand, biodegradable polymers can break down into raw materials of nature and disappear safely, relatively quickly, and reliably [32]. Biodegradable polymers can be divided into two groups according to their origin as it was shown in Table 2.1.

In applications like temporary therapeutic operations, there is a shift trend from the lasting biomaterials to biodegradable materials that can assist regeneration. The weighty causes of the change in the perception are the long-term biocompatibility problems, ethical and technical concerns related with revision surgeries for plenty of the permanent implants. Moreover, many flourishing biomedical branches such as; tissue engineering, regenerative medicine, gene therapy, controlled drug delivery and bio-nanotechnology increase the biodegradable materials demand [33].

Table 2.1
Biodegradable polymers examples.

Natural polymers	Synthetic polymers
Fibrin	Polylactic acid (PLA)
Starch	Poylglycolic acid (PGA)
Chitosan	Poly(lactic-co-glycolic acid) (PLGA)
Chitin	Polycaprolactone (PCL)
Hyaluronan	Polyorthoesters
Gluten	Polydioxanone
Collagen	Polyanhydrides
Gelatin	Polytrimethylene carbonate
Alginic acid	Polyphosphazenes
Cellulose	Polyhydroxybutyrate

Although biomedical polymers have lots of application field as mentioned [34]. They may possess some disadvantages as well. They may have a unsuitable surface chemistries for cell adhesion or degradation which can create high acidic concentration in environment to lead inflammatory response of the body [35]. Some of polymers with short degradation period can also degrade during implantation which may affect the final results. Biodegradable polymers should have some qualifications for implantation to avoid possible problems. The biodegradable polymers and the products of degradation should be non-toxic. They must be get rid of from the body in a desired speed. Moreover, during degradation, they should have sufficient mechanical properties [31, 33].

2.2 Polycaprolactone

Poly-ϵ-caprolactone (PCL) is a biodegradable polyester polymer. PCL is obtained from ring opening polymerization of caprolactone using a catalyst such as stannous octoate as illustrated at Figure 2.1. Caprolactone can be acquired by the oxidation of cyclohexanone. Lastly cyclohexanone is produced by the oxidation of cyclohexane, which is produced by reacting benzene with hydrogen. PCL undergoes hydrolytic

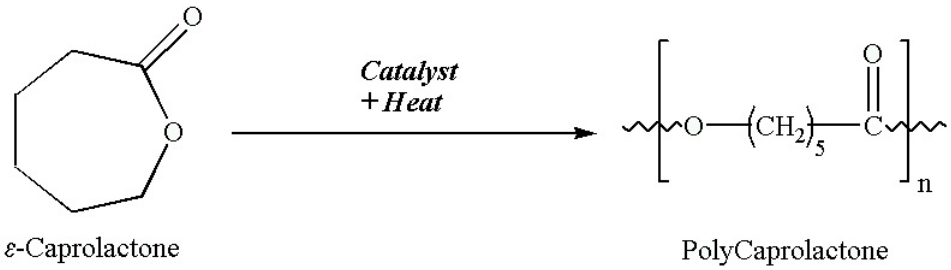

Figure 2.1 Ring-opening polymerisation of caprolactone to polycaprolactone [19].

degradation as a result of its weak aliphatic ester links against hydrolysis. Nonetheless, degradation process of PCL can take up to 4 years depending on its molecular weight and wetting property [12, 14]. PCL with more than 8 KDa molecular weight can not easily disperse through the semicyrstalline matrix, which accounting for the slow rate of PCL absorption in vivo [30]. Nevertheless, degredation period can be reduced by incorporation of co-polymers such as Polylactic acid (PLA). Making copolymer with other biodegradable aliphatic polyesters with PCL cause smaller oligomers formations which weaken the material.

As a semi-crystalline polymer PCL has a 60°C melting point, yet, it protect its molecular stability in high temperatures like 350°C [34]. At room temperature, PCL is formed as white solid, besides, above 60°C it becomes a pliable, transparent, putty-like material. In addition, it is soluble in a wide range of organic solvents. which gives PCL an easy shaping property. Moreover, Its non-toxic and bio-compatible qualifications makes PCL a convenient scaffold material option. The outputs of PCL degredation are hydroxycaproic acid, water and CO_2, and small polymer residuals which can be removed by phagocytosis of macrophages and giant cells [13, 33].

PCL is under evaluation as a drug delivery device in the form of porous microspheres. Moreover, it is used as biomaterial in the market in various forms and purposes;

- As an absorbable suture material PCL co-polymerised with glycolide is marketed as a monofilament suture by Ethicon, Inc. (Somerville, NJ), under the trade name Monacryl [36].
- For the treatment of the signs of aging, PCL are used as injectable fillers [37].
- Due to soft cartilage condition (tracheobronchomalacia) weak trachea in infants can cause airway collapse and respiratory insufficiency. A customized (the patient's airway shape), polycaptolactone tracheal splint is manufactured by the three-dimensional printer to treat this life-threatening condition [38].
- Last but not least, in neurosurgeries polycaprolactone implants can be used as burr-hole covers [39].

Besides its proved application fields, PCL is being examined as an option for vascular tissue applications. Seeding autologous endothelial cells on the surface of the material may help to avoid inconvenient blood-material interactions. However, hydrophobicity of PCL can lead to poor affinity for cell adhesion, thereby surface modification of PCL is needed to enhance adhesion and proliferation of cells especially for the blood-contacting materials [40].

2.3 Nanofibers

Biodegradable polymers can be prepared in different geometries according their purposes such as micro and nano particles [41], film membranes [42] and nanofibers [43]. Conventionally, fibers having diameters less than 1 μm can be classified as nanofibers [44]. Nanofibers exhibit a high surface area to volume ratio and degradation properties significantly different from those of the bulk films with the same sample thickness [34].

Nanofibrous scaffolds improve cellular functions more than traditional film scaffolds. Increased cellular attachment with fibroblasts [23], osteoblastic cells [24, 25], normal rat kidney cells [23], smooth muscle cells [26], neural stem cells [27] and embryonic stem cells [28] were reported for nanofiber meshes. Thus, nanofibers can be considered as a promising tool for tissue engineering to generate tissues quickly in comparison to film scaffolds. Yet, the information about the effects of nanofibers on cellular activity and tissue establishment are inadequate and nanofiber scaffold applications in tissue engineering are not very far from its starting point [45].

Table 2.2
Production techniques for nanofibers.

Name of Techniques
Phase separation
Drawing
Forcespinning
Melt blowing
Self assembly
Electrospinning

To produce nanofibers, different production methods have been developed. Some production techniques are subjected below as listed in Table 2.2.

- **Phase separation**: A small amount of solvent poured onto the polymer to

create a homogeneous polymer solution. After solvent removal porous nanofibrous structure is left. Prominent difficulties are controlling the distribution of structure (the pores can be not connected), need of toxic solvent and irregular structures [34].

- **Drawing**: Micropipette touch polymer solution droplet and while it moves away liquid fiber drawing occurs. The drawn fiber can be connected to another polymer solution droplet to form continuous fiber. However Controlling the fiber dimensions is not possible [46].

- **Forcespining**: This technique utilizes centrifugal forces to draw the material. The process begins by loading the solution/melt into a specially designed machine (spinneret). By the help of angular velocity the polymer is drawn [47].

- **Melt blown**: In melt blown technique the polymer is melted and ejected from extruder through a nozzle and drawing down the polymer with a jet of hot air. Only some polymers with high melt flow index can be produced below 1 micron diameter [48].

- **Self Assembly**: Self-assembly can be managed by pH-controlled, drying on surface induced or divalent-ion-induced methods. Fine fibers can be produced, However, length of fibers are also limited in this method. Moreover inability of fiber dimension control is another disadvantage of this technique [29].

- **Electrospining**: By the means of high potential difference and mostly the direct current,by the applying polymer solutions are drawn [49]. This method is chosen to produce Poly-ϵ-caprolactone nanofiber meshes. The subsequent section compromise the electrospining comprehensively.

2.4 Electrospining

Conventional spinning methods can not produce fibers with a diameter under 10 μm. On the other hand, nano scale fibers can be formed by electrospining technique.

More than 40 types of polymer can be used to produce nanofibers by electrospining. In this technique polymers must be in liquid phase. It can be molten or dissolved in a certain solution. The polymer is extruded from nozzles into strong electric field (5-30 kV gap) which is generated by direct current (DC). Due to high voltage, ions in the solution accumulate at the surface of the drop. The drop elongates and hemispheric surface of it forms a cone which is named as the Taylor Cone [34]. When electrical repulsive force overcomes the surface tension of charged the polymer liquid, electrical force creates the polymer jet and stretches it. As the force accelerates droplets of this liquid to the grounded target, the diameter of the fibers decreases. The liquid cools as it contacts with air, or when the solvent evaporates and eventually solidified as a fine fibers. However chaotic looping nature of the fibers cause a three dimensional non-woven mesh and this fiber cant be turned into woven or knitted structures [50]. Fabrics can be divided under three groups: knitted, weaved and non-woven. Physical orientations affect the materials' durability, stiffness and flexibility against external forces. The fabrics produced by electrospinning belong to non-woven group. In the future when positioning of every single fiber get controlled, it will be possible to mimic tissue environment more with non-woven materials.

Electrospinning systems consist of three major units: a high voltage power supply, polymer pomp with a nozzle (needle, pipette tip) and a grounded collecter (metal plate, rotating cylinder). Generally the polymers are dissolved in some solvents before electrospinning to form a polymer solution at liquid phase [51, 52].

The electrospinning process is managed by many parameters such as; solution parameters (concentration, viscosity, conductivity, molecular weight, and surface tension) process parameters (applied electric field, tip to collector distance, and feeding or flow rate) and ambient parameters [52]. These parameters are investigated below.

Effects of Electrospinning Parameters:

1. **Concentration of Polymer Solution:** In the electrospining, low concentration polymer solutions cause beads on fibers and high concentration polymer solutions are not able to maintain the flow, therefore formation of continuous fibers are hindered [53, 52].

2. **Molecular Weight of Polymer:** Low molecular weight polymer solutions tend to form beads and a high molecular weight solutions provide fibers with larger diameters. Moreover, in a low polymer concentration, high molecular weight can help to sustain a necessary solution viscosity to produce a uniform polymer jet [53, 52].

3. **Viscosity of Polymer Solution:** Viscosity is correlated with polymer concentration and molecular weight of polymer. Low viscosity cause discontinuous fiber formation, and in high viscosity, ejection of polymer solution jets become troublesome. [53, 52].

4. **Surface Tension:** Different solvents have different surface tension values. High surface tension of a solution can cause inconsistent polymer jets and lead fiber beads formation. Lower surface tension let us work with of a lower electric field in electrospinning [52].

5. **Conductivity of Polymer Solution:** Solution conductivity is essentially based on the polymer type, the solvent, and salts (if any exist). Mostly polymers are conductive in the high voltage field, with a few exceptions. The ions increase conductivity of the solution. Adding ionic salts like KH_2PO_4, NaH_2PO_4, and NaCl helps to produce beadless fibers and increased uniformity within fibers. High solution conductivity leads to decrease in the diameter of the electrospun nanofibers however, in the existence of strong electric field it also cause bending instabilities which leads a wider range of diameter distribution. Low solution conductivity may generate beads in nanofibers [52].

6. **Applied Voltage:** It is pointed out, the diameter of the produced fibers are decreasing by the stretching forces under the applied high potential difference.

However, type of the polymer concentration of the solution, the distance between the collector and the nozzle cause variations at the fiber diameter. This makes the effect of voltage a controversial issue [52].

7. **Flow Rate:** Increasing the polymer flow rate leads higher fiber diameter or even beaded fibers due to lack of required drying time. Low flow rates are more preferable as it provides sufficient time for the solvent evaporation before attaining the collector [52].

8. **Type of Collectors:** Collector is a conductive substrate where the nanofibers are clustered. The fiber alignment is determined by the type of the collector and its rotation speed. Many type of collectors for the need of various applications such as; conductive papers, conductive cloths, wire meshes, parallel or gridded bars, rotating rods, rotating wheels, liquid non solvent coagulation bath are in use [52].

9. **Nozzle to Collector Distance:** Optimum distance between the tip and collector can be managed considering the evaporation of solvent from the nanofibers. If the distance is either too close or too far, beads show up. Moreover, close distances may cause production of flatten fibers [52].

10. **Ambient Parameters:** Solution temperature between 25 to 60 °C leads decreasing in the viscosity of the polymer solutions, thus, fiber diameter decreasing can be occurred. At high humidity, small circular pores on the surface of the fibers can be observed. At low humidity, polymer solution may dry faster, on the other hand clogged needle tip problem arises, below a certain level [52].

11. **Solvents for Polymers:**The solvents used in electrospinning of polymers can effect many solution properties such as conductivity. For example dimethylformamide (DMF) is a dipolar solvent, which has a high dielectric constant and dipole moment. Addition of DMF in to solution enhances the solution conductivity which is a supportive feature for fabrication of fibers without bead. Desired solvent properties are good vapor pressure, low boiling point and, maintaining the integrity of the polymer solution. Different solvents may introduce different

surface tensions and accordingly considerable effects on fiber diameter can be observed [52].

2.5 Histidine

20 natural amino acids are considered as the building blocks of proteins. In this group, histidine is a basic and essential amino acid with a positively charged imidazole functional group. The unique behaviors of histidine were discussed in literatures from different aspects [54]. It can take the most diverse roles in the protein architectures due to its special molecular structure which was shown in Figure 2.2 [55, 56, 57].

Table 2.3
Properties of histidine amino acid.

Properties	Values
pK $_a$ of (α)-Carboxyl Group	1.8
pK $_a$ of (α)-Amino Group	9.2
pK $_a$ of (α)-Ionizing Side Chain	6.0
Residue Mass (daltons)	137.15
Occurrence in Proteins (mol%)	2.1

Table 2.3 shows pK_a values for side chains of free histidine amino acid. When histidine incorporated into proteins, the pK_a is raised to 7.0 ± 0.4 . Because of the imidazole group of histidine side chain can exchange hydrogen near physiological pH. It often takes a role coordinating ligand in metallic cations, act as a hydrogen bond donor, and acceptor in many enzymatic catalysis [58, 59].

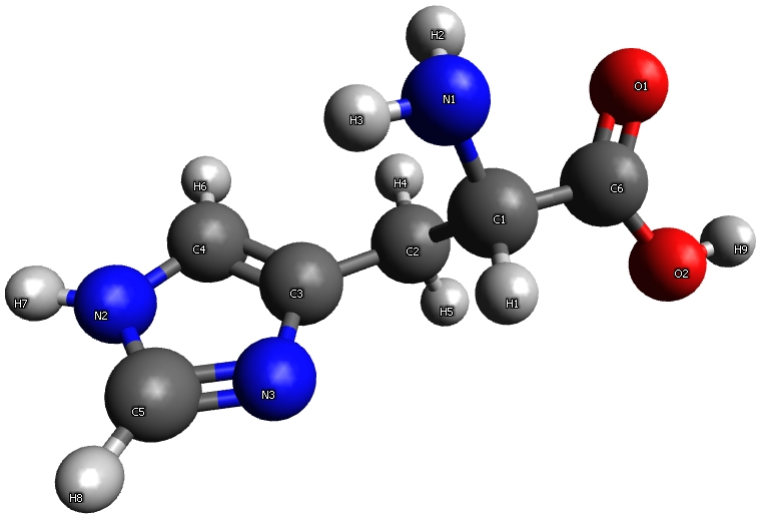

Figure 2.2 Molecular formula of histidine.

2.6 Fetuin

Fetuin is one of the blood plasma proteins in the fetal and early postnatal period of many mammals. Fetal calf serum have more fetuin protein than albumin yet it is present in the plasma of adults with only low expression levels. Besides, fetuin can be exist in the extracellular matrices, in a wide variety of developing organs including lung, kidney, skeletal muscle, cartilage bone and, the central and the peripheral nervous system [60].

Despite many efforts, knowledge of functional role about fetuin in the developing nervous system and/or any other tissue is very limited. It is known to be present and made in the liver which assist the attachment and spreading of cells in a culture medium [61]. It is a glycoprotein which contains sialic acid like laminin. Fetuin is factor in preventing pathological mineralization and calcification. Further functions may include insulin signaling and modulation of transforming growth factor (TGF)-β activities (proliferation, cellular differentiation), thus, fetuin has an important role in the development of neurons in embryonic period [62].

A number of studies are showed that fetuin is a promoter for the tumor cell growth. However, the role of fetuin in in-vitro studies is controversial due to its' ability to interact with many adhesive proteins. Moreover, in a study malignant Lewis lung carcinoma cells have reduced growth potential in fetuin-A. In highly tumorigenic cells, the growth promoting potential of fetuin-A depending on the particular circumstances can provide both favorable and unfavorable microenvironments for tumor growth [63].

3. MATERIALS AND METHODS

3.1 Synthesis of Poly-ϵ-caprolactone (PCL) Nanofibers by Electrospinning

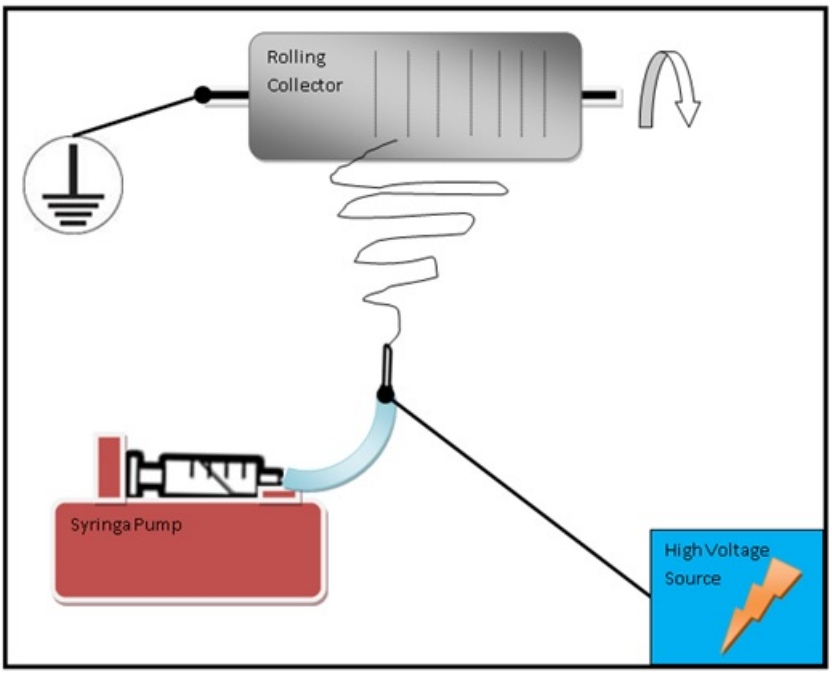

Figure 3.1 Schematic representation of electrospinning procedure.

A schematic of the electrospinning process is shown in Figure 3.1. 10ml, 10% (w/v) Poly-ϵ-caprolactone (Mn=70,000-90,000) solution was used in every run. DMF was used, to increase conductivity of THE polymer solution and chloroform was used as the main solvent in the solution with a 1/4 (v/v) ratio [64]. It was poured into a 20 ml syringe, equipped with 26 gauge needle. All chemical materials were supplied from Sigma-Aldrich. The electrospinning machine (NE 300, Inevenso, Turkey) was used with a collector surface rolling cylinder target. The electrospining device set to 25 kV of potential difference between the electrodes and the distance between them was kept constant at 15 cm. Rotation speed of collector cylinder with 8 cm diameter was kept at 435 rpm and flow rate of the solution was set to 10 ml/hr. The polymer jet accelerated towards the grounded collector and deposited on the aluminum foil in the form of a porous nonwoven fabric.

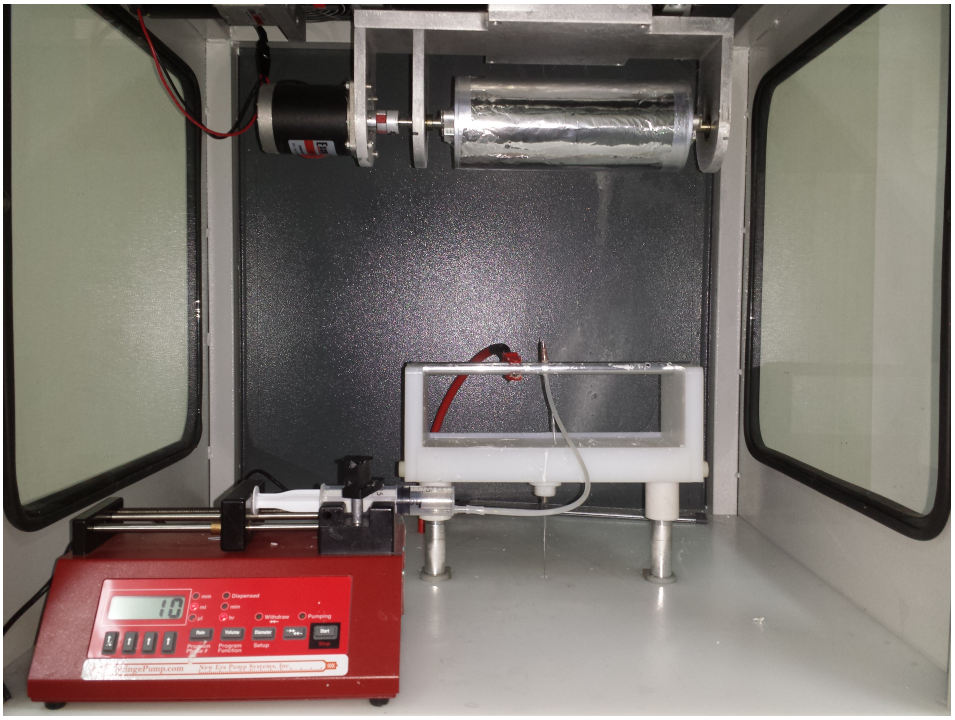

Figure 3.2 Image of invenso NE 300 electrospinning instrument.

3.2 Modification of Poly-ϵ-caprolactone Surfaces

10 % (w/v) $(C_6H_{10}O_2)_n/CH_3Cl$) Poly-ϵ-caprolactone (Mn=70,000-90,000) solution, was cast on smooth metal substrates to obtain plain PCL membranes. Over 48 hours of evaporation period, PCL membranes were obtained. Dried PCL membranes and nanofiber meshes were cut into specimen size of 1.5 cm diameter rounds for the subsequent surface reactions. Membrane and nanofiber specimens immersed in glass bottle of 10 % (g/l) Hexamethylenediamine (HMDA)/isopropanol concentration of the solutions for overnight.The aminolyzed PCL samples washed in distilled water for 24h at room temperature to remove unreacted HMDA [65].

Equal mole of histidine, cyanamide, and N-hydroxysuccinimide (NHS) were used in immobilization reactions. To activate histidine, varying amount histidine, cyanamide, N-hydroxysuccinimide were dissolved according to the (His/HMDA) mole ratios which were 1/1;1/2;1/4 in 0.1 mol MES (2-(N-morpholino)ethanesulfonic acid)

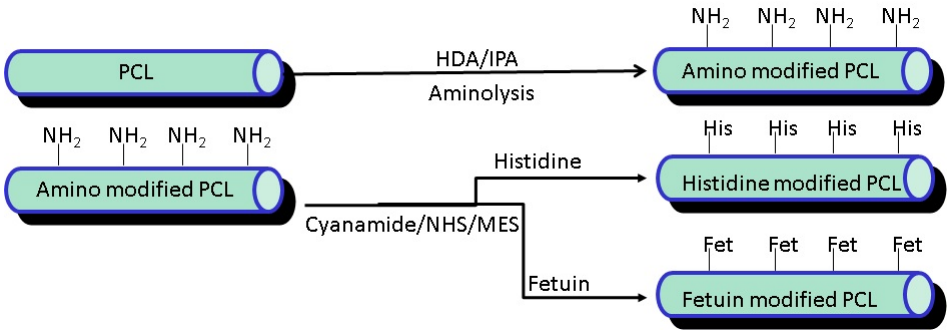

Figure 3.3 Modification of PCL membranes and nanofiber meshes.

sodium salt buffer. To activate fetuin, 0.06g fetuin, 1 mole cyanamide, 1 mole NHS dissolved in 20 mL PBS (phosphate buffered saline) buffer.

3.3 Characterization of PCL Membranes and Nanofiber Meshes

3.3.1 Optical Microscope

Optical Microscope was used to examine fiber diameters on glass slides. For the microscope imaging, flat collector of electrospining device was used to stick microscope slides on. In total, 66 nanofiber samples were randomly selected for the measurement.

3.3.2 Scanning Electron Microscope (SEM)

Surface topography of the PCL membranes and nanofiber meshes (unmodified, HMDA modified, histidine immobilized (with 1:1,1:2,1:4 histidine:HDMS mole ratios) and fetuin immobilized) were examined by Scanning Electron Microscopy (SEM) (Philips XL30 ESEMFEG/EDAX) at Bogazici University Research and Development Center Electron Microscopy and Microanalysis Unit. Membranes' surfaces were coated with Pt using Polaron SC7640 Sputter Coater, operated at 1.6 kV, 15-20 mA for 60 seconds prior to SEM analysis.

3.3.3 Contact Angle Measurements

Surface wetting properties of modified and unmodified PCL nanofiber membranes were measured by using contact angle measurement device (DSA 100, Krüss GmbH, Germany) in order to evaluate the hydrophobicity of the substrates. The initial drop volume was 10 μl and the dosing rate was set at 10 μl/min for each measurement.

3.3.4 Fourier Transform Infrared Spectroscopy (FTIR)

Fourier Transform Infrared Spectroscopy (FTIR) spectrum were obtained by using Nicolet 520 spectrophotometer. FTIR spectrum were recorded over the range of 4000 to 400 cm^{-1} with 32 scans in order to investigate the chemical compositions of PCL membranes and nanofiber meshes (unmodified, HMDA modified, histidine immobilized (with 1:1,1:2,1:4 histidine:HDMS mole ratios) and fetuin immobilized).

3.3.5 X-ray Photoelectron Spectroscopy (XPS)

To characterize chemical compositions of PCL and nanofiber meshes (unmodified, HMDA modified, histidine immobilized (with 1:1,1:2,1:4 histidine:HDMS mole ratios) and fetuin immobilized) Thermo Scientific K-Alpha X-ray Photoelectron Spectrometer (XPS) was used. Monochromatic aluminum K(α) radiation was operated, at 72 W, 400 μm spot size, 90°C angle and with a 128-channel detector.

3.4 In Vitro Degradation Studies

In order to understand the degradation characteristics of PCL nanofiber and histidine immobilized PCL nanofiber, by means of weight loss degradation study performed. 3 square samples with 1cm^2 of area were prepared from histidine immobilized nanofiber and unmodified nanofiber meshes. Samples were kept in 24-well plate within

2 mL pH 7.4 PBS solution at 37°C in the incubator for 28 weeks. Every week samples were weighted once again. Before the measurements samples were wiped and dried in 40°C in the incubator for 1,5 hour.

3.5 Cell Culture Studies

Cell proliferation on modified PCL membranes and nanofibers meshes (experimental groups were given at Table 3.1) was evaluated by MTT assay (3-(4, 5-dimethylthiazol-2-y1)-2, 5-diphenyltetrazolium bromide), a yellow tetrazole using L929 mouse fibroblast cells [66]. Briefly, $1X10^4$ cells were seeded on 24 well plates containing Dulbecco's modified Eagle's medium (DMEM), 10% Fetal bovine serum (FBS) and 0.5% penicillin/streptomycin antibiotic solution. Cells were exposed to the PCL membranes and nanofiber meshes for 48 h at 37°C in 5% CO_2. After the 48 hours of incubation, the medium on PCL membranes and nanofibers meshes was removed, washed with PBS three times, and then 500 μl DMEM and 75 μl of 5 mg/ml MTT were added to each well containing L929 cells mouse fibroblast cells. The 24-well plate was then incubated at 37°C in a humidified atmosphere of 5 % CO_2 for 4 h, followed by removing the mixed solution of medium and MTT, adding 300 μl 2-propanol (acidified with 0.04 M HCl) of to each well, pipetting up and down to dissolve crystals in a condition without the presence of light. Finally the solutions were transferred to a plate reader for absorbance measurements at 595 nm using microplate reader (iMark, Biorad, USA).

Table 3.1
Experimental Groups.

Experimental groups in cell studies
TCPS
PCL membrane
HMDA modified PCL membrane
His modified PCL membrane (1/4 His/HMDA mol ratio)
His modified PCL membrane (1/2 His/HMDA mol ratio)
His modified PCL membrane (1/1 His/HMDA mol ratio)
Fetuin modified PCL membrane
PCL Nanofiber Mesh
HMDA modified PCL nanofiber mesh
His modified PCL nanofiber mesh (1/4 His/HMDA mol ratio)
His modified PCL nanofiber mesh (1/2 His/HMDA mol ratio)
His modified PCL nanofiber mesh (1/1 His/HMDA mol ratio)
Fetuin modified PCL nanofiber mesh

4. RESULTS

4.1 Synthesis of Electrospun Poly-ϵ-caprolactone Nanofiber Meshes and Membranes

10% (w/v) Poly-ϵ-caprolactone (Mn=70,000-90,000) solution dissolved in chloroform (CH_3 Cl) was used in every run for the preparation of PCL nanofiber meshes. Applied voltage, needle-collector distance were kept constants at 25 kV and 15 cm, respectively. PCL membranes were prepared with the same concentration as PCL nanofiber meshes by solvent casting method after 2 days of evaporation process. Photos of electrospun nanofiber meshes and membranes were shown in Figure 4.1.

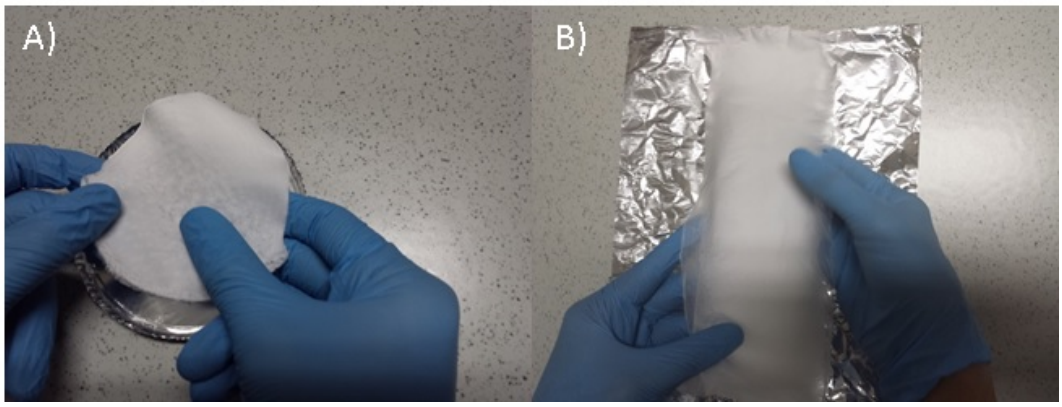

Figure 4.1 Images of PCL membranes a) plain membrane b) electrospun mesh.

In order to determine the diameter distribution of PCL nanofibers, a histogram was obtained by using SEM and optical images of electrospun nanofiber meshes. Histagram, SEM and optical images of PCL nanofibers were given in Figure 4.2 and 4.3. Mean value of 66 samples were measured and average diameter of PCL nanofibers was found to be 1,05 μm $\pm$ 0.519 .

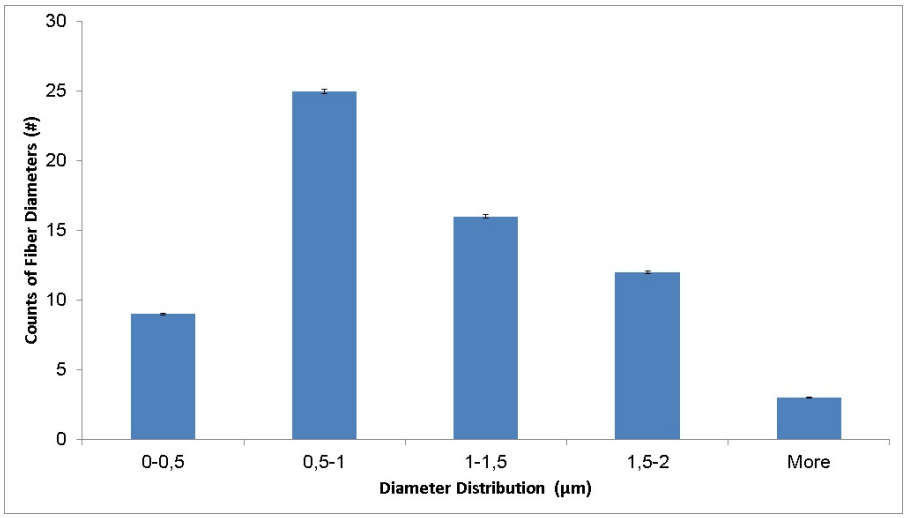

Figure 4.2 Histogram of PCL nanofiber diameters.

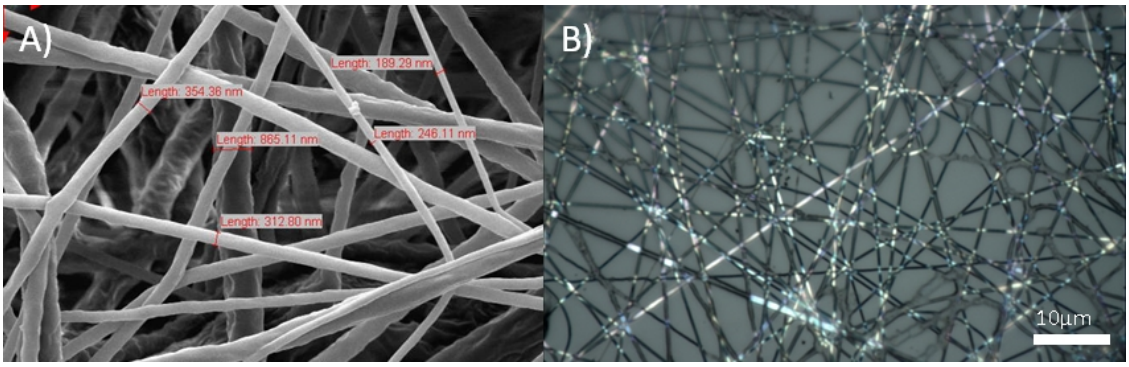

Figure 4.3 Images of PCL nanofibers a) SEM; b) optical image microscope.

4.2 SEM Images of Poly-ϵ-caprolactone Membranes and Nanofiber Meshes

As mentioned in experimental section, we have performed multistep modification onto both PCL membranes and nanofiber meshes in order to improve their biocompatibilities and adjust their biodegradabilities. SEM micrographs of PCL membranes and nanofiber meshes are shown in Figure 4.4 and 4.5, respectively. According to the SEM images it was clearly observed that unmodified PCL membranes have higher porous structure than the histidine and fetuin modified membranes.

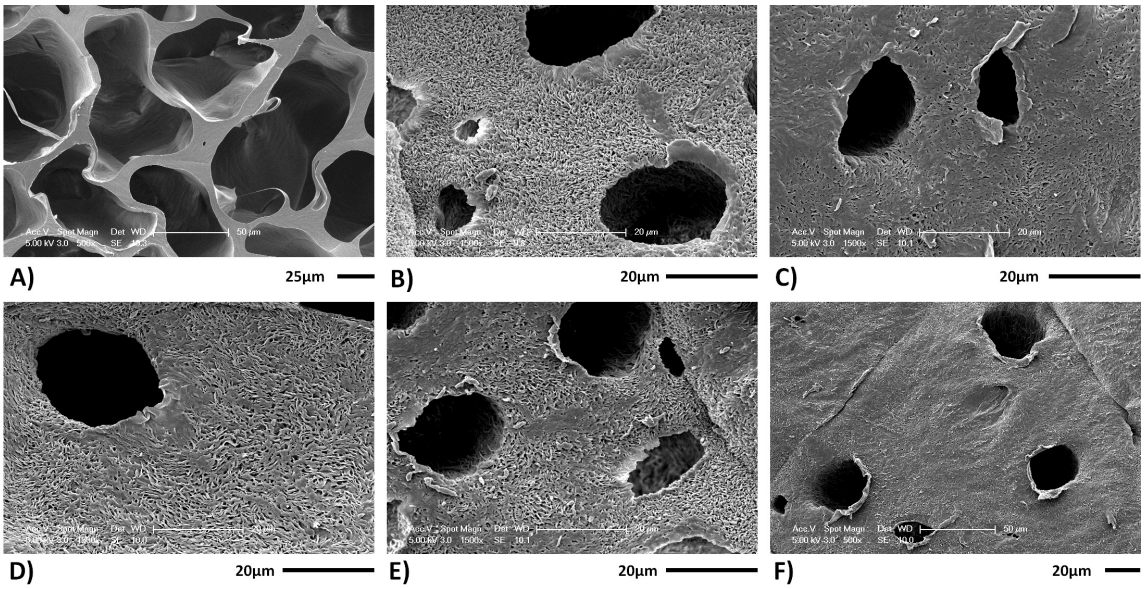

Figure 4.4 SEM images of PCL membranes (PM). a) unmodified PM; b) HMDA modified; c) histidine (His) modified (1/4 His/HMDA mol ratio); d) His modified (1/2 His/HMDA mol ratio); e) His modified (1/1 His/HMDA mol ratio); f) fetuin modified.

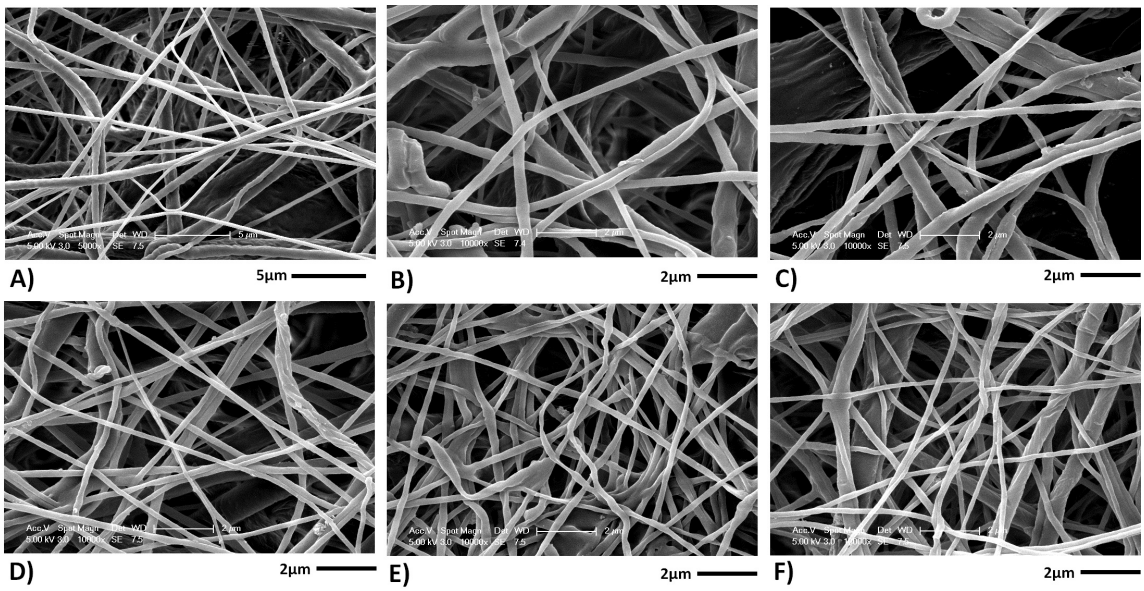

Figure 4.5 SEM images of PCL nanofiber meshes(NF). a) unmodified NF; b) HMDA modified; c) histidine (His) modified (1/4 His/HMDA mol ratio); d) His modified (1/2 His/HMDA mol ratio); e) His modified (1/1 His/HMDA mol ratio); f) fetuin modified.

Electrospun PCL nanofiber morphology was also imaged by SEM. Most of the fiber diameters were below μm range and was found to be 1,05μm $\pm$ 0,519. There was no significant change on the fiber diameter and mesh structure after the modification step with, HMDA, histidine and fetuin.

4.3 Contact Angle Measurements of Histidine and Fetuin Modified Poly-ϵ-caprolactone Nanofiber Meshes

Static water contact angle values of HMDA modified, histidine and fetuin immobilized PCL nanofiber meshes were determined and given in Table 4.1. Hydrophobicity of PCL nanofiber meshes decreased after modification with histidine an fetuin biomolecules as expected. Water contact angles of HMDA, histidine and fetuin immobilized PCL nanofiber meshes were found lower than unmodified PCL nanofiber meshes. The water contact angles of PCL decreased from 80.67 $\pm$ 0.51 to 63.63 $\pm$ 0.67, 61.37 $\pm$ 1.19, 63.40 $\pm$ 1.64, respectively.

Table 4.1
Contact angle measurement of PCL nanofiber meshes.

Samples	Contact Angle (^{o})
Poly-ϵ-caprolactone (PCL)	80.67 $\pm$ 0.51
Hexamethylenediamine Modified PCL	63.63 $\pm$ 0.67
Histadien Immobilized PCL	61.37 $\pm$ 1.19
Fetuin Immobilized PCL	63.40 $\pm$ 1.64

4.4 FT-IR Spectra of Modified Poly-ϵ-caprolactone Nanofiber Meshes

ATR-FTIR was used to investigate the chemical functional groups that were present on the surfaces of the PCL nanofiber meshes after modification with HDMA, histidine and fetuin. Results are given in the Figures 4.6-4.8. In each spectrum figure,

Table 4.2
Characteristic FTIR bands of PCL.

Chemical Bonds	FTIR band (wave number, cm^{-1})
Asymmetric CH_2 stretching	2949
Symmetric CH_2 stretching	2865
Carbonyl stretching C=O	1727
C-O and C-C stretching in the crystalline phase	1293
Asymmetric C-O-C stretching	1240
Symmetric C-O-C stretching	1170

To observe the bands after each modification step clearly, difference spectrum was recorded. FT-IR bands of PCL are listed in Table 4.2. These peaks were observed in the FT-IR spectrum in Figure 4.6. The bands at 2943 cm^{-1}, 2866 cm^{-1}, 1725 cm^{-1}, 1294 cm^{-1} 1239 cm^{-1} and 1165 cm^{-1} wave numbers are the traces of asymmetric CH_2 stretching, symmetric CH_2 stretching, carbonyl stretching, in the crystalline phase C-O and C-C stretchings, asymmetric C-O-C stretching and symmetric C-O-C stretching, respectively [67, 68].

Characteristic carbonyl ester (Table 4.2) band of PCL was observed at 1725 cm^{-1}. After modification with HMDA, the carbonyl ester peak was broadened and shifted to lower wavenumber, 1721 cm^{-1} because of new amide band formation through aminolysis reaction. There were no signals due to the N-H stretching of the amido groups but there was a shifted the carbonyl (C=O) stretching of the amide linkage related signals was observed at 1652 cm^{-1} on (expected 1640 cm^{-1}) the difference spectrum which is an evidence of the reaction of HMDA with PCL. Additionally, the observation of a small sharp band in the range of 3000-3600 cm^{-1} at the HMDA spectrum corresponding to the N-H stretching of the NH_2 groups further confirmed the successful introduction of HMDA on PCL nanofiber meshes.

Characteristic carbonyl ester band of PCL was also observed at 1725 cm^{-1} before histidine and fetuin immobilization. After histidine and fetuin immobilization carbonyl peaks were shifted to 1726 cm^{-1} and 1733 cm^{-1}, respectively. To prove

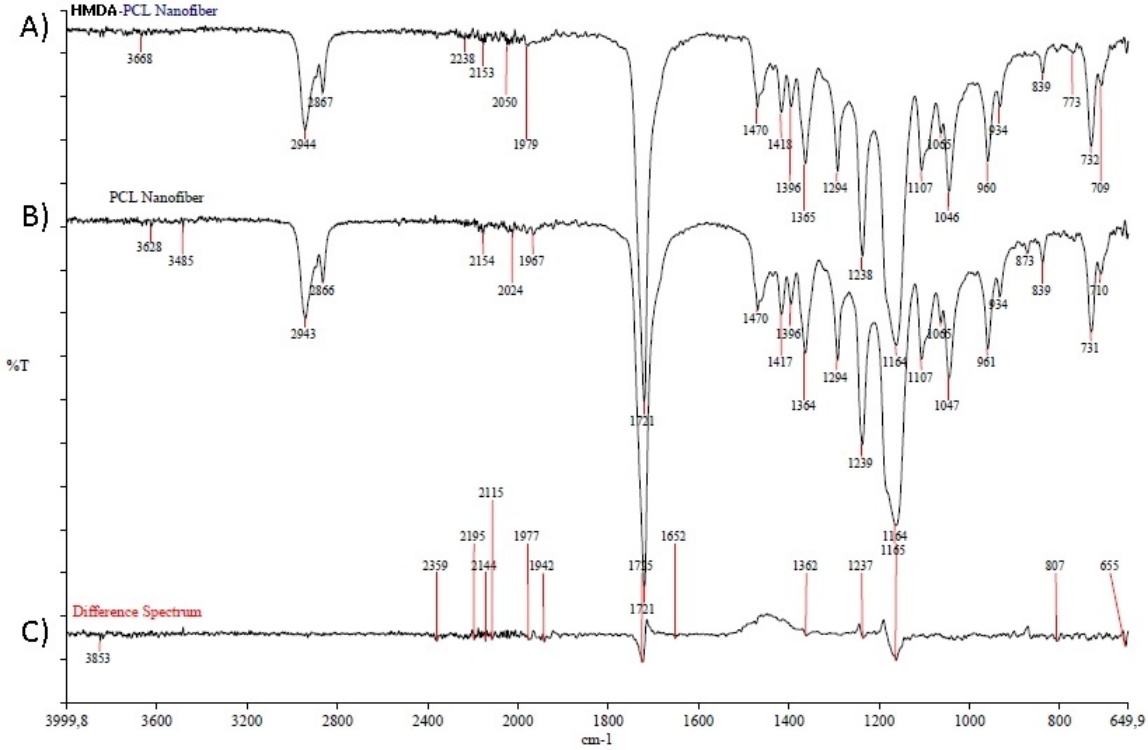

Figure 4.6 FTIR spectra of HMDA modified nanofiber mesh. a) HDMA modified; b) non-modified; c) difference of both spectra.

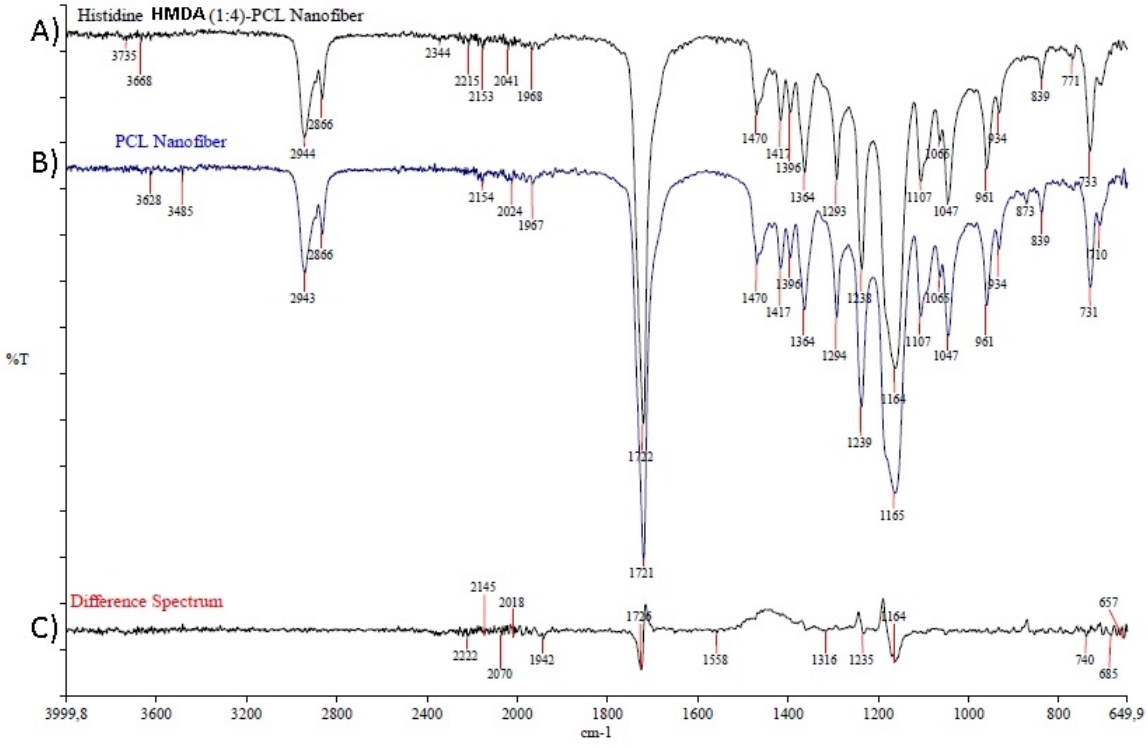

Figure 4.7 FTIR spectrum of histidine immobilized PCL nanofiber mesh. a) histidine immobilized; b) non-modified; c) difference of both spectra.

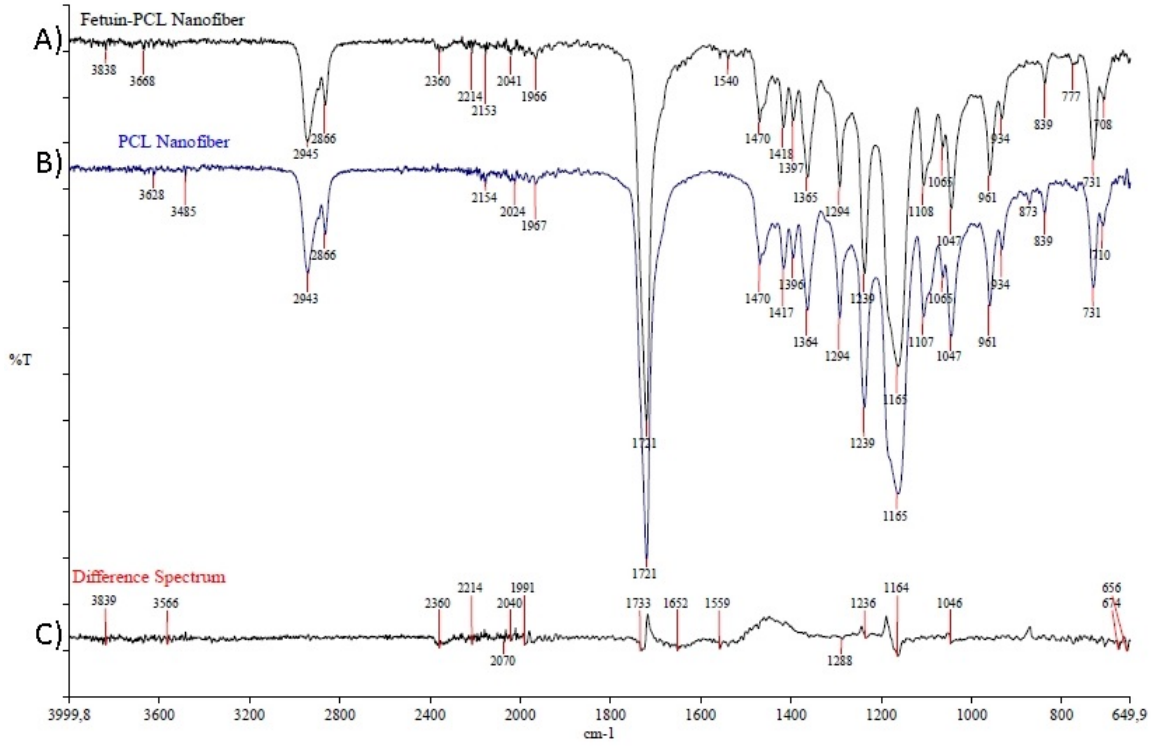

Figure 4.8 FTIR spectrum of fetuin immobilized PCL nanofiber mesh. a) fetuin immobilized; b) non-modified; c) difference of both spectra.

at 1558 cm^{-1}, the band stemmed from vibrations of imidazole ring of histidine was observed. That is a confirmation for the successful histidine immobilization and also fetuin immobilization, two bands at 1652 cm^{-1} and 1559 cm^{-1} in the spectrum of fetuin immobilized PCL meshes were recorded which correspond to amide I and amide II bands.

4.5 XPS Analyzes of Poly-ϵ-caprolactone Membranes and Nanofiber Meshes

4.5.1 XPS Analyzes of the plain and HMDA modified PCL membrane

Chemical functional groups on the surfaces of both Poly-ϵ-caprolactone (PCL) membrane and the modified PCL membrane were analyzed by using Thermo Scientic K-Alpha XPS.

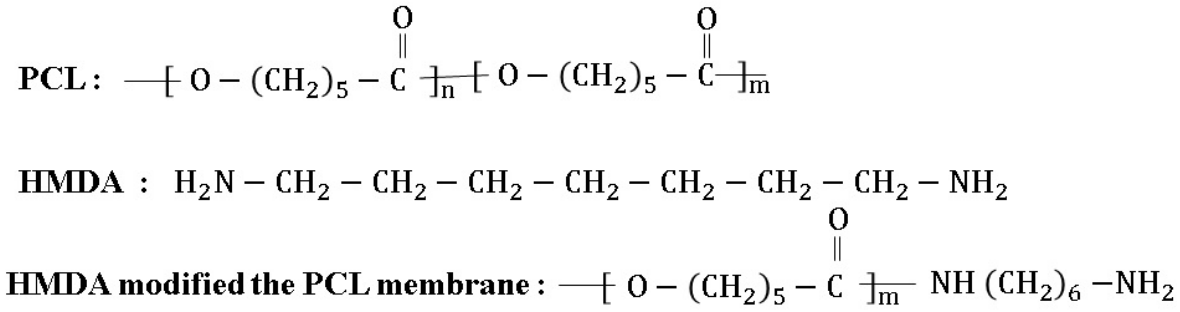

Figure 4.9 Chemical formulas of PCL, HMDA, and HMDA modified PCL molecules.

The XPS analyzes were performed to demonstrate the C1s, O1s levels of plain PCL membrane (Figure 4.10a) The deconvoluted XPS spectra of the C1s region of PCL plain membrane was shown that C-H/C-C, C-O, and O=C-O peaks were characterized at 284.47 eV, 286.07 eV and 288.51 eV, respectively (Figure 4.10e). The analysis of XPS survey spectrum of hexamethylenediamine (HMDA) modified PCL membrane was shown in the Figure 4.10b. High-resolution N1s spectra for PCL plain membrane and HMDA-modified PCL membrane was shown in the Figure 4.10c. In the analysis of N1s core level, two new peaks at 399.32 eV and 401.24 eV can be attributed to C-NH_2 and O=C-NH bonds, respectively (4.10d). The deconvolution of C1s spectra was appeared at 284.53 eV, 285.89 eV, and 288.46 eV, attributable to C-H/C-C, C-N/C-O, and O=C-O/O=C-NH peaks, respectively and was shown in the Figure 4.10f.

The XPS survey spectrum of PCL nanofiber mesh was presented in the Figure 4.11a. High resolution spectra were examined by using detail structure of a peak to get information about chemical constitutions of atoms. In the analysis of C1s core level, C-H/C-C, C-O and O=C-O peaks were found at 284.69 eV, 286.11 eV, and 288.63 eV, respectively and shown in Figure 4.11e. The presence of aminolysis in the PCL nanofiber meshes was also confirmed by XPS survey spectrum. The XPS survey spectrum of HMDA-modified PCL nanofiber meshes was shown in the Figure 4.11b. High-resolution N1s spectrum for PCL nanofiber meshes and HMDA-modified PCL nanofiber meshes was shown in the Figure 4.10c. The analysis of N1s core level spectrum was appeared at 399.59 eV and 401.85 eV, in respect to C-NH_2 and O=C-NH bonds Figure 4.11d. The C1s core level spectrum indicates the successful introduction

of amine groups (-NH_2) on the PCL structure. The C1s core-level spectra of the HDMA-PCL nanofiber meshes was resolved into four peak components at 284.49 eV, 285.14 eV, 286.1 eV and, 288.54 eV, which are assigned to C-H/C-C, C-N , C-O and O=C-O/O=C-NH, respectively (Figure 4.11f).

4.5.2 XPS Analysis of Histidine modified HMDA-PCL membrane and meshes

The XPS survey spectra of histidine (1:1, 1:2, and 1:4 His:HMDA mole ratio) modified PCL membranes were also analyzed by using Thermo Scientific K-Alpha XPS. According to the XPS survey spectrum of histidine (1:1, 1:2, and 1:4 His:HMDA mole ratio) modified PCL membranes, C1s, N1s and O1s peaks obtained from the analysis was shown in the Figure 4.13a The high resolutions of C1s , N1s and O1s of 1:1, 1:2, and 1:4 histidine modified PCL were shown in Figure 4.13 (b,c,d).

The C1s spectrum of histidine (1:4 His:HMDA mole ratio) modified PCL membrane can be curve fitted into four different peaks that were found the binding energies at about 284.41 eV, 284.9 eV, 285.88 eV, and 288.46 eV inrespect to C-H/C-C, C=C, C-N /C-O and O=C-NH/O=C-O bonds (Figure 4.14). The analysis of N1s core level spectra was observed at 399.76 eV, 399.37 eV and 401.33 eV, in respect to C-N, aromatic N imidazole ring, and NH-C=O peak and was shown in the Figure 4.14.

The deconvolutions of C1s spectra and N1s spectra of histidine (1:2 His:HMDA mole ratio) modified PCL membrane was resolved into four different peaks at 284.5 eV, 285.33 eV, 286.12 eV and 288.48 eV, corresponding to C-H/C-C/C=C , C-N , C-O, and O=C-NH bonds. The analysis of N1s core level spectrum was appeared at 398.83 eV and 400.02 eV, and assignable to N=C-NH and N-C=O peak.

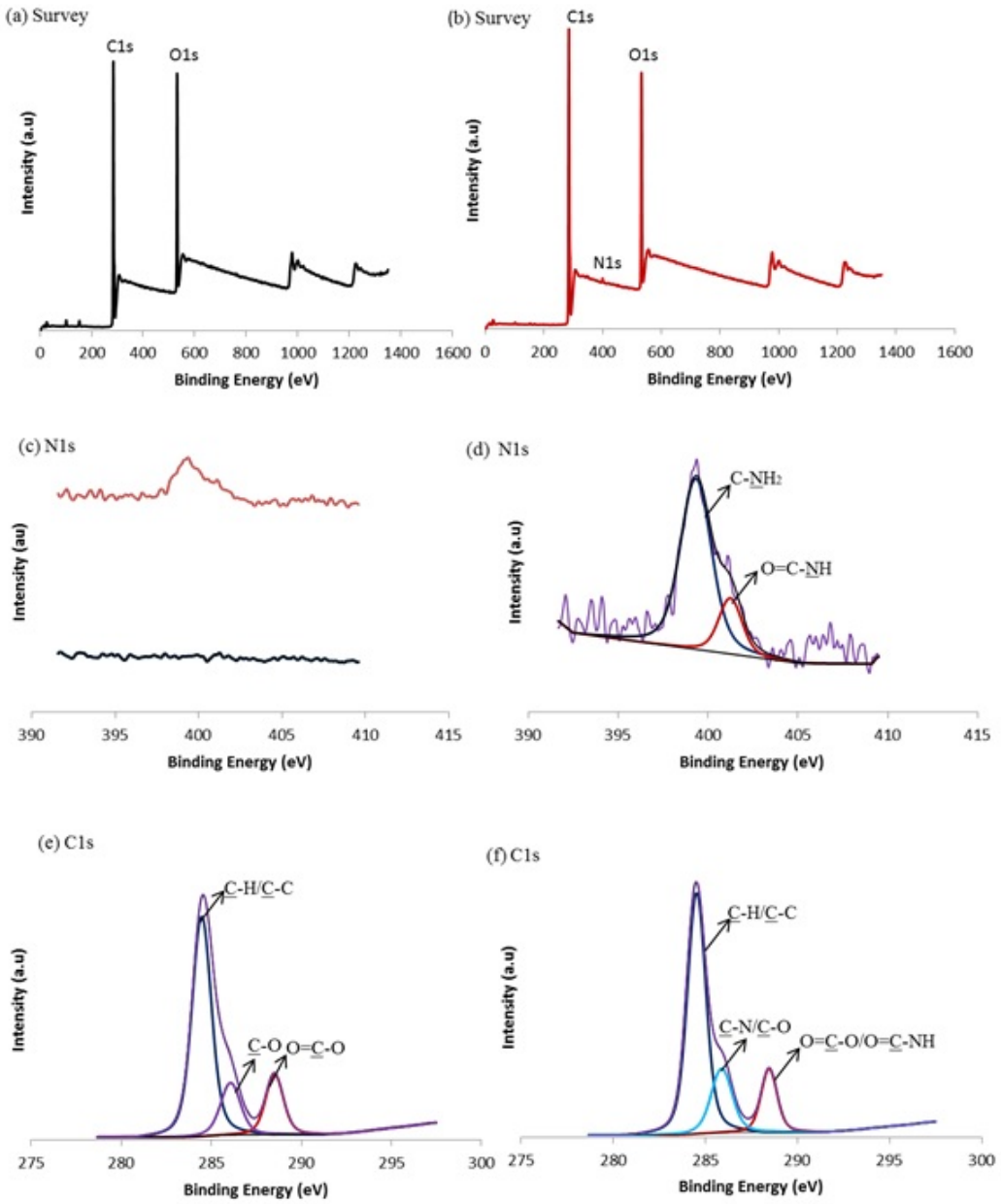

Figure 4.10 XPS survey spectrum of the a) plain PCL membrane b) HMDA modified PCL membrane c) the raw data spectrum of N1s spectra of PCL plain membrane (black line) and HMDA modified PCL membrane (red line) d) deconvolution of the N1s core level spectra of HMDA modified PCL membrane e) deconvolution of the C1s core level spectra of PCL membrane f) deconvolution of the C1s core level spectra of HMDA modified PCL membrane.

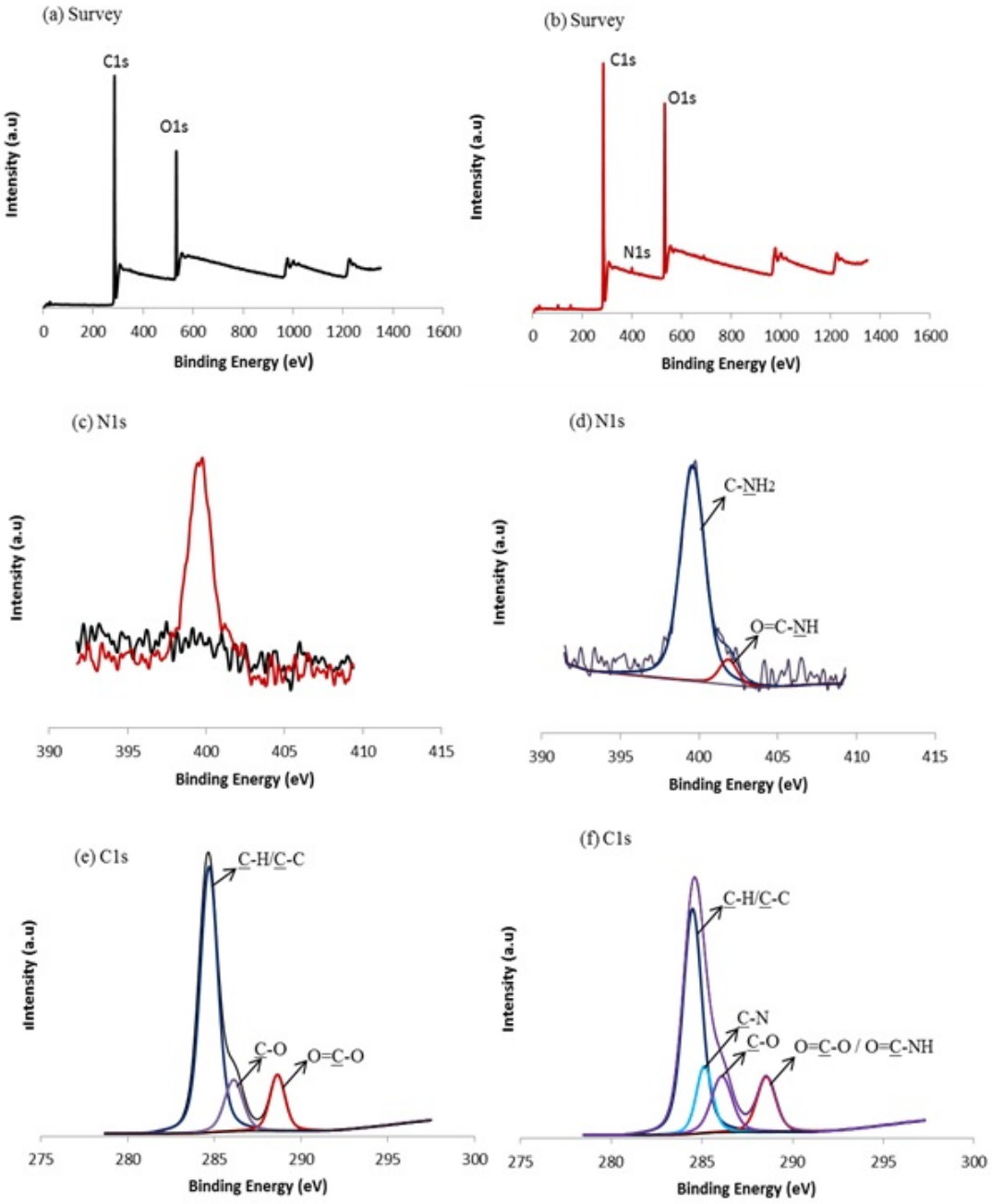

Figure 4.11 XPS survey spectrum of the a) PCL nanofiber mesh b) HMDA modified PCL nanofiber mesh c) the raw data spectrum of N1s spectra of PCL nanofiber mesh (black line) and HMDA modified PCL nanofiber membrane (red line) d) deconvolution of the N1s core level spectra of HMDA modified PCL nanofiber mesh e) deconvolution of the C1s core level spectra of PCL nanofiber mesh f) deconvolution of the C1s core level spectra of HMDA modified PCL nanofiber mesh.

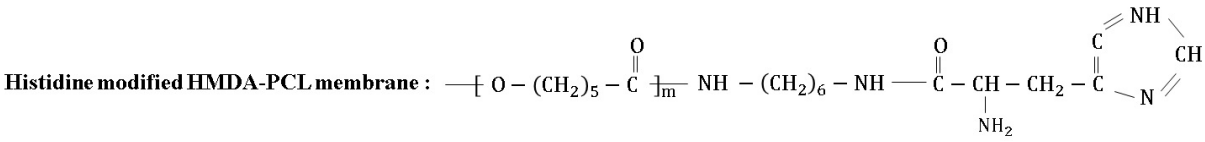

Figure 4.12 Chemical formula of histidine modified PCL polymer.

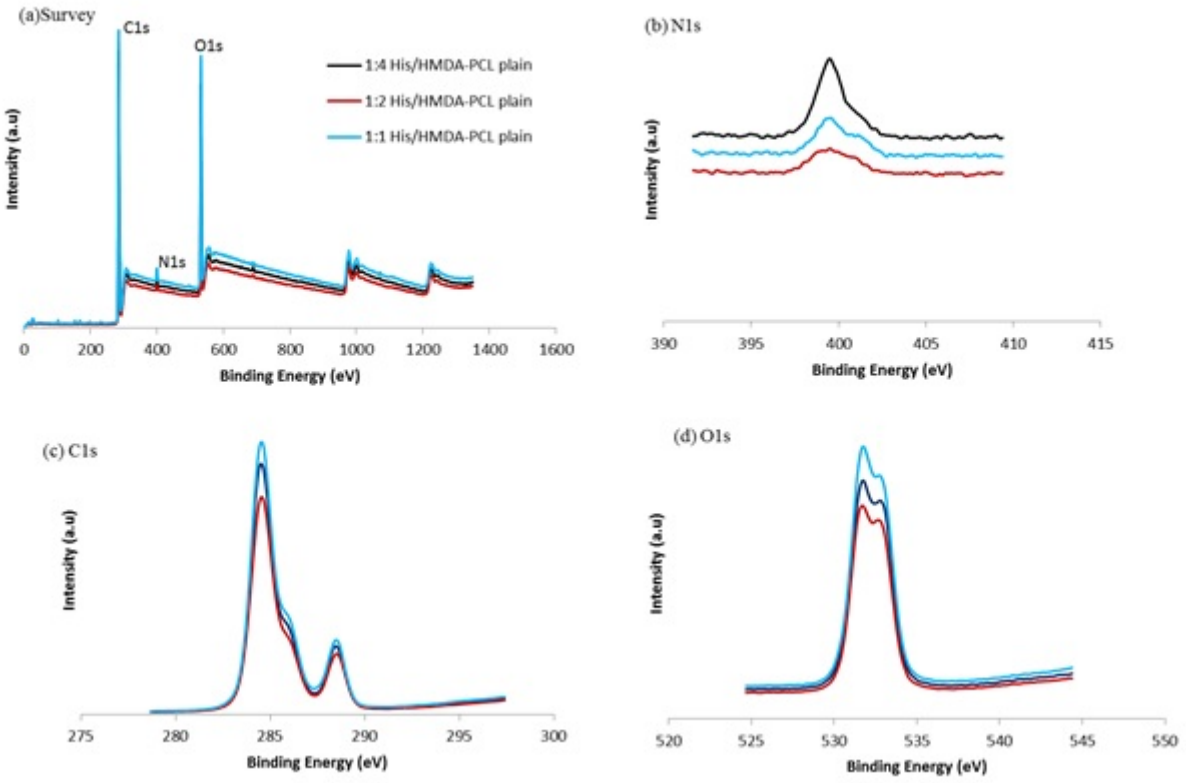

Figure 4.13 The XPS survey spectra and a) N1s b), C1s c) and O1s d) core level spectra of 1:1 (blue line), 1:2 (red line), and 1:4 (black line) histidine modified PCL membranes.

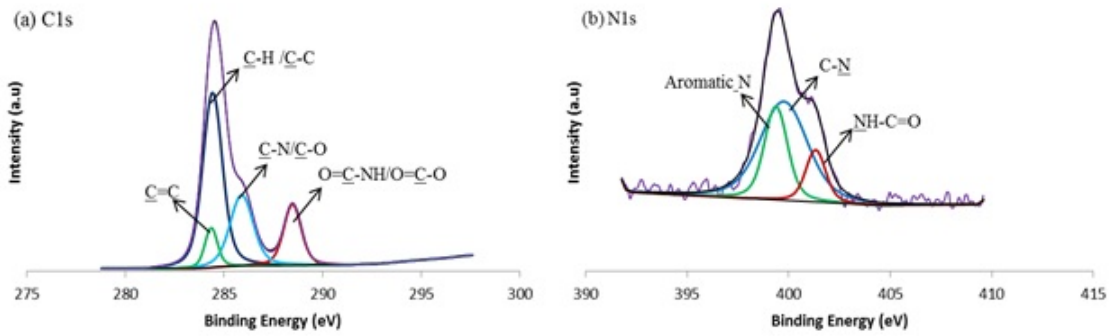

Figure 4.14 a) Deconvolution of the C1s core level spectra of histidine (1:4 His:HMDA mole ratio) modified PCL membrane b) deconvolution of the N1s core level spectra of histidine (1:4 His:HMDA mole ratio) modified HMDA-PCL plain membrane.

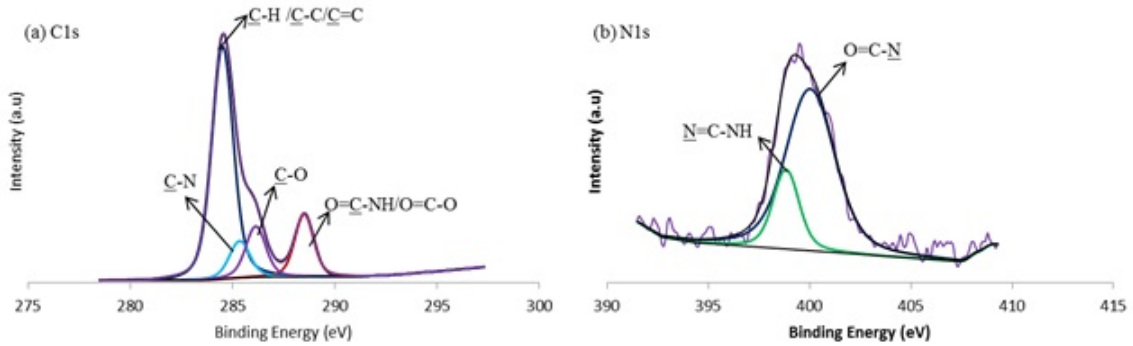

Figure 4.15 a) Deconvolution of The C1s core level spectra of histidine (1:2 His:HMDA mole ratio) modified PCL membrane b) deconvolution of the N1s core level spectra of histidine (1:2 His:HMDA mole ratio) modified PCL membrane.

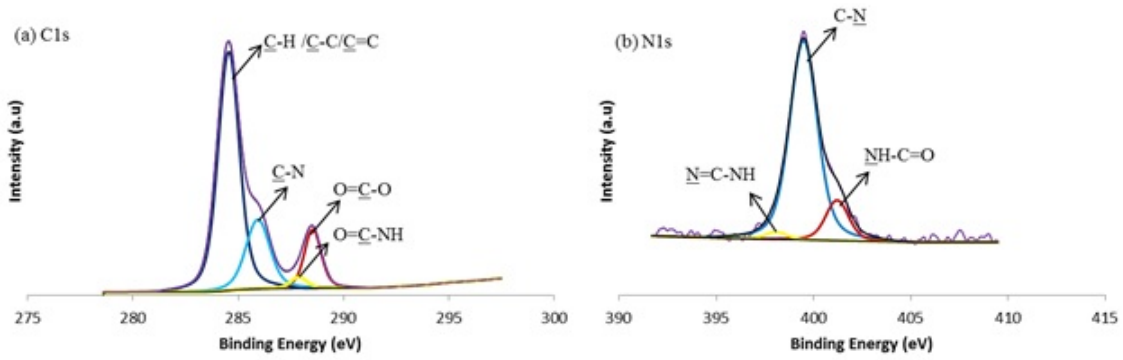

Figure 4.16 a) Deconvolution of the C1s core level spectra of histidine (1:1 His:HMDA mole ratio) modified PCL membrane b) deconvolution of the N1s core level spectra of histidine (1:1 His:HMDA mole ratio) modified PCL membrane.

The C1s spectrum of histidine (1:1 His:HMDA mole ratio) modified PCL membrane can be curve fitted into four different peaks that were shown the binding energies at about 284.55 eV, 285.92 eV, 287.87 eV and 288.53 eV, the assignable to C-H/C-C/C=C, C-N/C-O, O=C-NH and O=C-O bonds. (Figure 4.16). After peak fitting of the N1s core-level spectrum, three deconvoluted peaks were observed at 398.08 eV, 399.48 eV and 401.21 eV, attributable to, N=C-NH, C-N and NH-C=O peak (Figure 4.16).

The XPS analysis for C1s, O1s and N1s levels of histidine (1:1, 1:2, and 1:4 His:HMDA mole ratio) modified PCL nanofiber meshes was also examined by using Thermo Scientific K-Alpha XPS and was shown in Figure 4.17.

The deconvolution of C1s spectra of histidine (1:4, His:HDMA mole ratio) modified PCL nanofiber meshes was analyzed in which, C=C, C-H/C-C, C-N/C-O, O=C-NH and O=C-O bonds were found at 284.05 eV, 284.63 eV, 286.02 eV, 287.98 eV,and 288.63 eV, respectively as shown in Figure 4.18. The raw data spectrum of N1s can be curve fitted with three components at 399.52 eV, 400.47 eV and 400.71 eV, corresponding to C-N, N=C-NH and NH-C=O shown in the Figure 4.18.

The C1s spectrum of histidine (1:2, His:HDMA mole ratio) modified PCL nanofiber meshes can be curve fitted into five different peaks that were shown the binding ener-

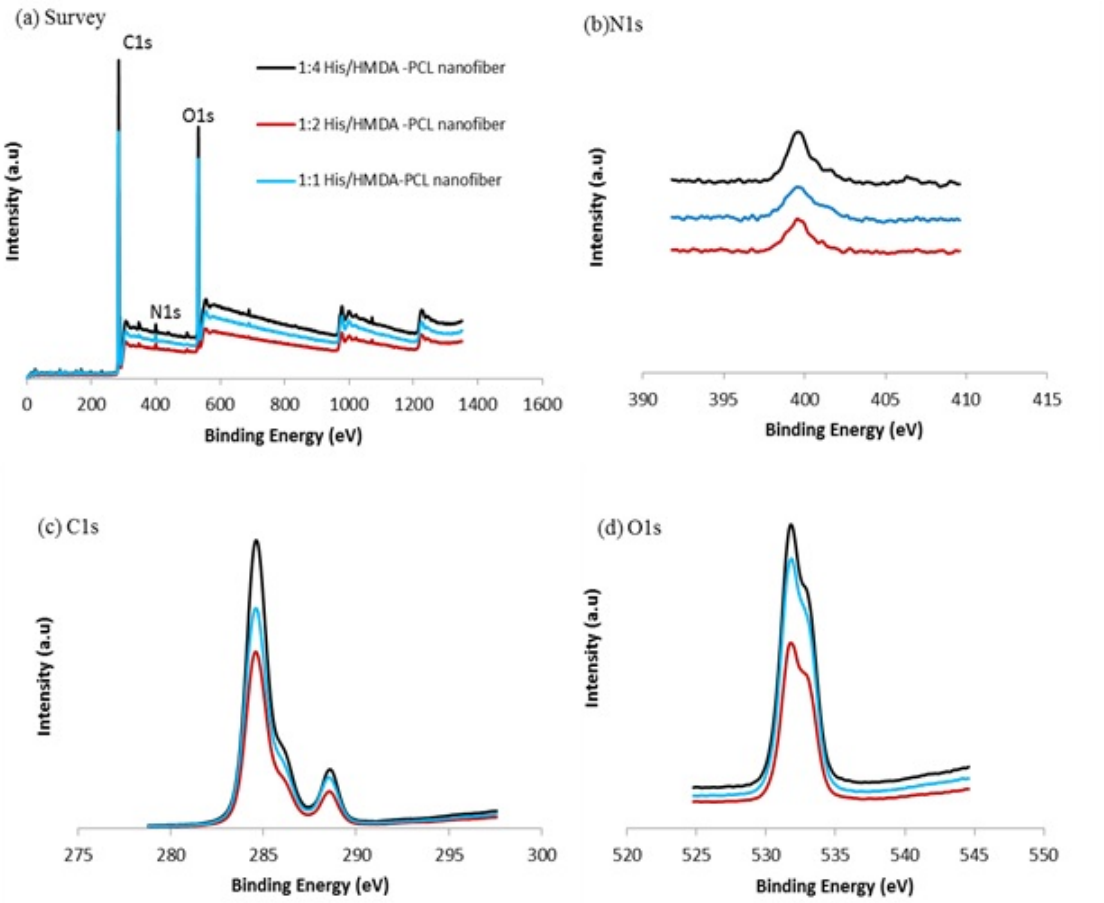

Figure 4.17 The XPS survey spectra a) and N1s b) , C1s c) and O1s d) core level spectra of 1:4 (His:HDMA mole ratio) (black line), 1:2 (His:HDMA mole ratio) (red line), and 1:1 (His:HDMA mole ratio) (blue line) histidine modified PCL nanofiber meshes.

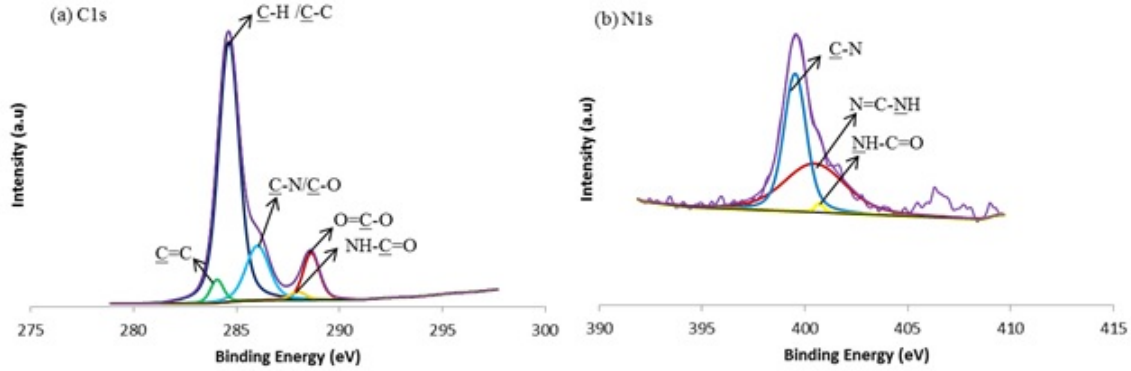

Figure 4.18 a) Deconvolution of the C1s core level spectra of 1:4 histidine modified HMDA-PCL nanofiber mesh b) deconvolution of the N1s core level spectra of 1:4 histidine modified HMDA-PCL nanofiber mesh.

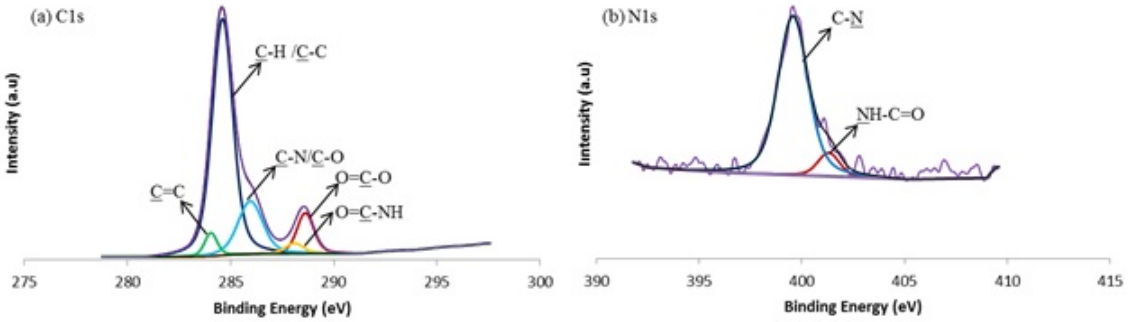

Figure 4.19 a) Deconvolution of the C1s core level spectra of histidine (1:2, His:HDMA mole ratio) modified PCL nanofiber meshes b) deconvolution of the N1s core level spectra of histidine (1:2, His:HDMA mole ratio) modified PCL nanofiber meshes.

gies at about 284.05 eV, 284.61 eV, 285.96 eV, 288.09 eV and 288.63 eV corresponding to C=C C-H/C-C, C-N/C-O, O=C-NH and O=C-O bonds as shown in Figure 4.19. In the analysis of N1s core level, NH-C=O and C-N bonds found at 401,3 eV and 399,56 eV were shown in the Figure 4.19

Figure 4.20 has shown that the C1s spectrum of histidine (1:1, His:HDMA mole ratio) modified PCL nanofiber meshes can be curve fitted into five different peaks as 284.49 eV, 285.07 eV, 286.06 eV, 287.66 eV and 288.56 eV, attributable to C-H/C-C, C-N, C-O, O=C-NH and O=C-O bonds respectively. The analysis of N1s core level was appeared at 399.56 eV and 401.52 eV binding energies attributable to C-N and NH-C=O bonds

4.5.3 XPS Analysis of Fetuin modified PCL membranes

The XPS survey spectrum of fetuin modified HMDA-PCL plain membrane for C1s, O1s and N1s levels was measured by using Thermo Scientific K-Alpha XPS and shown in the Figure 4.21. The C1s, O1s and N1s core level spectra of fetuin modified PCL membranes were measured and shown in the Figure 4.21.

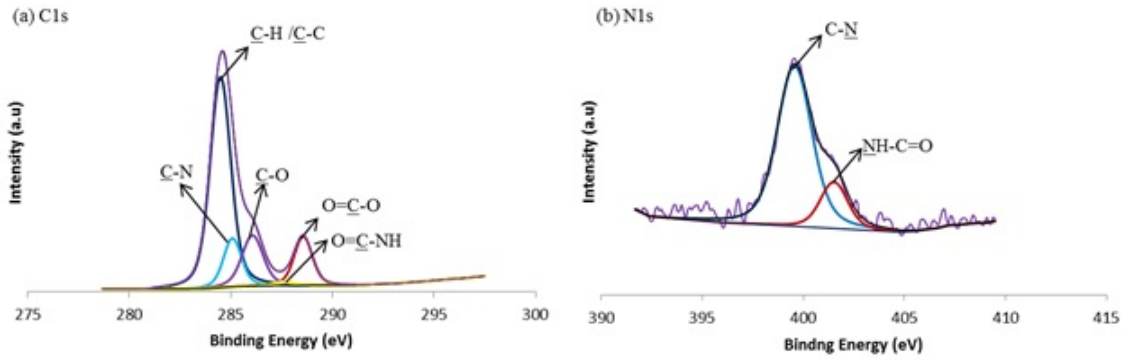

Figure 4.20 a) Deconvolution of the C1s core level spectra of histidine (1:1, His:HDMA mole ratio) modified PCL nanofiber meshes b) deconvolution of the N1s core level spectra of histidine (1:1, His:HDMA mole ratio) modified PCL nanofiber meshes.

As can be seen from the Figure 4.21, the C1s core level can be resolved into five peaks at binding energies of 284.34 eV, 284.93 eV, 285.81 eV, 287.5 eV and 288,41 eV, corresponding to C-H/C-C, C=C, C-N/C-S/C-O , O=C-N and O=C-O peaks. After peak fitting of the N1s core-level spectrum, three deconvoluted peaks were appeared at 399.36 eV, 400.82 eV and 401.66 eV, corresponding to C-N, O=C-N and C-NH bonds respectively.

The XPS survey specturum of the C1s, O1s and N1s core level spectra of fetuin modified PCL membranes was analyzed by using Thermo Scientific K-Alpha XPS and shown in the Figure 4.22. The deconvoluted high resolution spectrum of the C1s peak of fetuin modified PCL membranes were analyzed by six main peaks. The analysis of C1s core level was observed at 284.41 eV, 284.96 eV, 285.88 eV, 287.72 eV and 288.55 eV, the corresponding to, C-H/C-C, C=C, C-N/C-O/C-S ,O=C-N and O=C-O (Figure 4.22). The new possible band (C=S) in the spectrum revealed that fetuin modification was successful. The analysis of N1s core level spectrum was appeared at 399.48 eV and 401.16 eV the corresponding to C-N and O=C-NH, respectively (Figure 4.22).

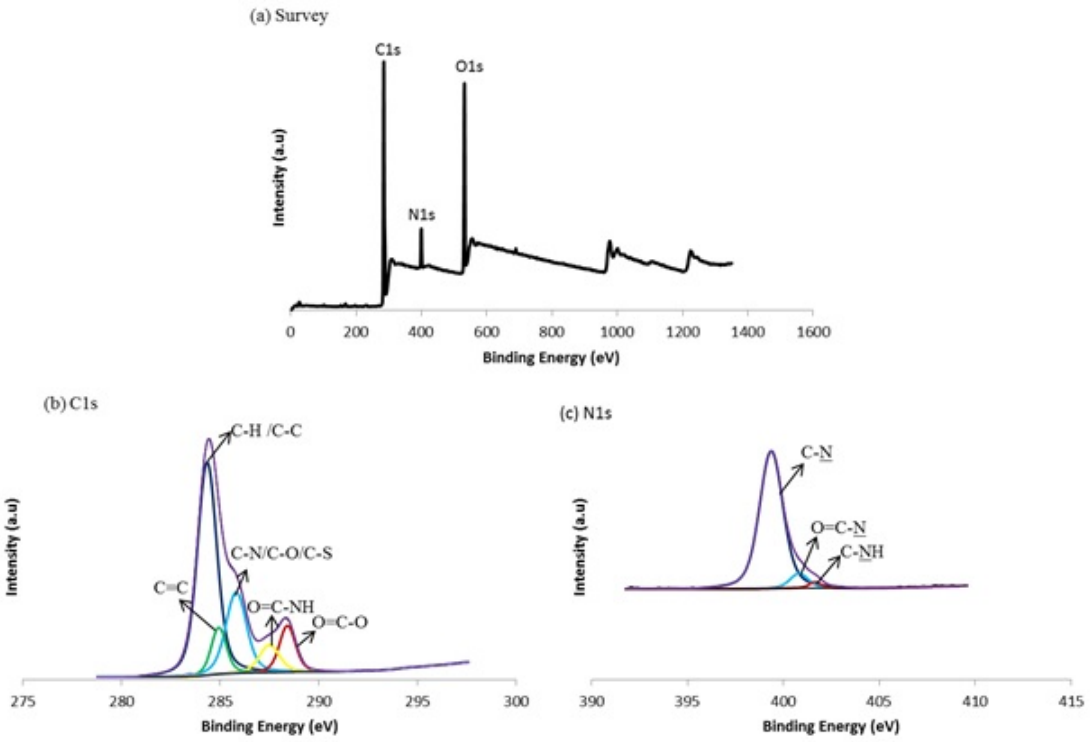

Figure 4.21 XPS survey spectrum of the a) fetuin modified PCL membrane b) deconvolution of the C1s core level spectra of fetuin modified PCL membrane c) deconvolution of the N1s core level spectra of fetuin modified PCL membrane.

4.6 Degradation Studies

In vitro degradation of unmodified and histidine modif n PCL nanofibers were evaluated by weight loss determination in PBS buffer for 28 weeks at 37°C. The weight loss of unmodified and histidine modified substrates as a function of the degradation time was given in Figure 4.23. There was no significant change in the weight of both unmodified and histidine modified nanofibers after 7 months.

4.7 Cell Proliferation Test

In order to understand viability enhancements effect on the membranes, MTT test was applied on modified and unmodified PCL membranes. Proliferation of L929 fibroblast cells on PCL membranes and nanofiber meshes at 48 hours were determined by using MTT assay (Figure 4.24, 4.25). Unmodified PCL membranes showed similar

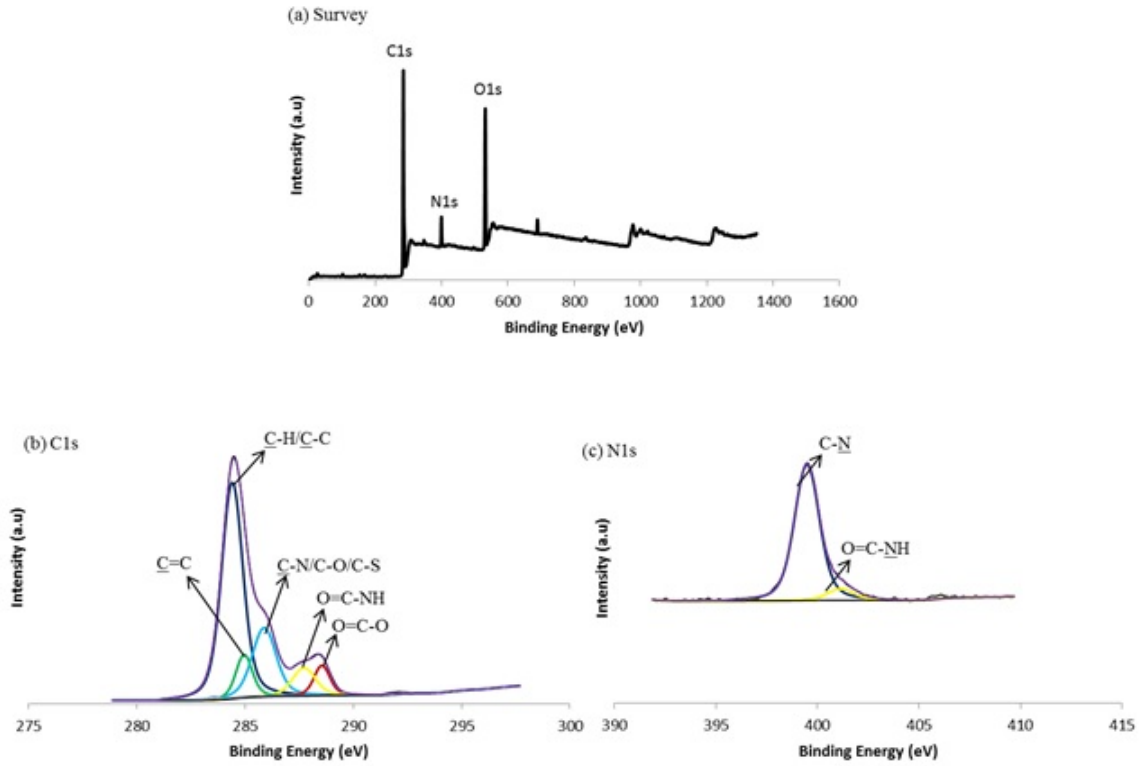

Figure 4.22 XPS survey spectrum of the a) fetuin modified PCL membrane b) deconvolution of the C1s core level spectra of fetuin modified PCL membrane c) deconvolution of the N1s core level spectra of fetuin modified PCL membrane.

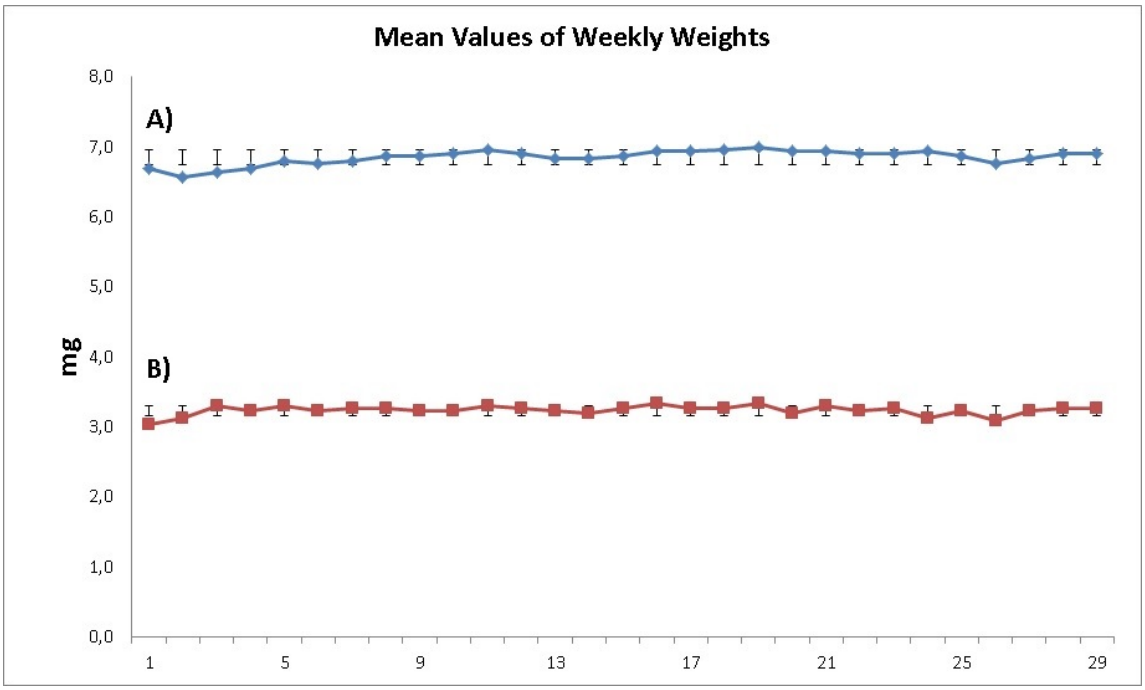

Figure 4.23 Weight loss of a) unmodified and b) histidine modified PCL nanofibers.

cell growth ability (94.5 ± 2.5%) as the control groups. The number of cells on HDMA modified PCL membranes decreased to 69.3 ± 4.7% with respect to control groups.

Cell proliferation on histidine amino acid modified PCL membranes was increased from 111.3 ± 5.3% to 127.6 ± 3.3% with an increasing His:HMDA mole ratio, respectively. 83.2 ± 1.9% proliferation was observed on fetuin immobilized PCL membranes. On unmodified PCL nanofiber meshes cell proliferation percent was found to be 102.1 ± 1.8. The number of cells on HMDA modified PCL membranes decreased to 79.7 ± 2.6% with respect to control groups. Cell proliferation percent was increased from 126.9 ± 5.4 to 158.7 ± 5.1 on histidine modified PCL nanofibers with an increasing histidine content, PCL/HMDA/His 4:1; PCL/HMDA/His 1:1 mole ratio. 89.2 ± 3.6 percent proliferation was observed on fetuin immobilized PCL nanofiber meshes. According to the MTT assay, histidine modified PCL nanofiber meshes were shown better cell proliferation percents than PCL membranes with an increasing histidine content.

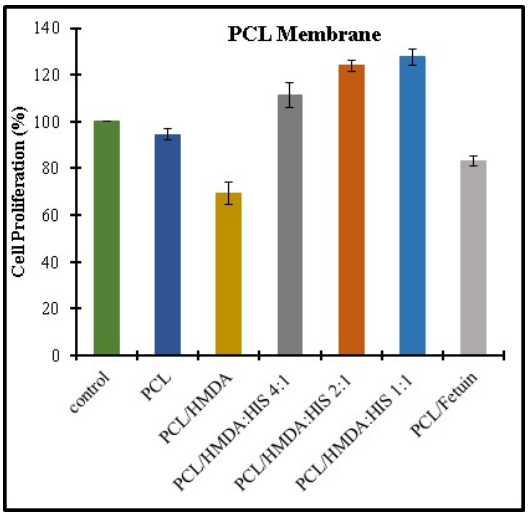

Figure 4.24 Results of the MTT assay: cell proliferation on the histidine and fetuin modified PCL membranes after 48 h exposure.

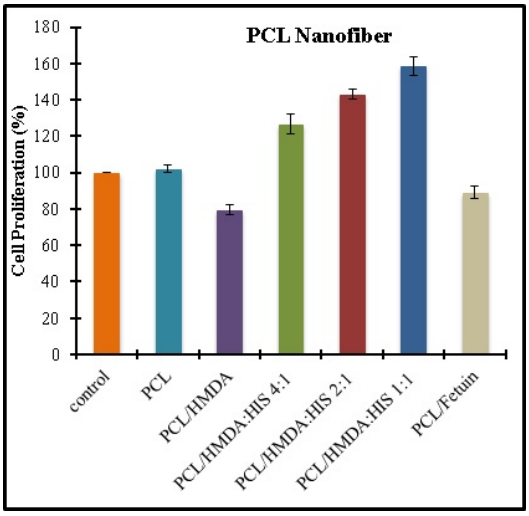

Figure 4.25 Results of the MTT assay: cell proliferation on the histidine and fetuin modified PCL nanofiber meshes after 48 h exposure.

5. DISCUSSION

5.1 Synthesis of Electrospun Poly-ϵ-caprolactone Membranes and Nanofiber Meshes

Polycaprolactone is relatively cheap, easily accessible material which has approvals for implantation usages [12, 13]. It has a a significant long degradation time which can lasting up to 4 years [12, 14] previously. Therefore, it is popular on the long term implantation applications [15]. The successful introduction of cell cultures in a porous PCL matrix has been reported [16, 17]. On the other hand PCL is not a perfect polymer, in terms of cytocompatibility. Thus, to enhance cytocompatibility, modification of PCL is necessary [18].

For this purpose, in this thesis to enhance biocompatibility histidine amino acid and fetuin were chosen as model modifiers. Histidine was chosen because of having a positively charged imidazole functional group where it plays the most diverse roles in the protein architectures [58, 59] and fetuin protein which is one of the blood plasma proteins that assists the attachment and spreading of cells [69].

Nano scale PCL fibers were synthesized by electrospinning technique that it is one of the easiest and the cheapest way of production of nanofibers [70, 71]. In this purpose, electrospinning process was used to produce nanofibers from PCL solution. Since the definition of the nanofibers was explained by Podgarski et al. and Zhou et al., all the fibers with a diameter less than 1 μm are identified as nanofibers [70, 72]. Therefore, it is possible to say that the fibers which were classified as electrospun in this thesis were nanofibers. The median diameter of the deposited fibers are in the range of 0.5 μm to 1 μm (Figure 4.3 - 4.5).

PCL membranes were synthesized by solvent casting technique [73, 74]. According to SEM images (Figure 4.4) unmodified PCL membranes have shown higher pore

structure than the histidine and fetuin modified PCL membranes. This may be due to possible recasting with isopropanol which was used for the aminolysis reaction. On the other hand this behavior did not observe in PCL nanofiber meshes (Figure 4.6). This situation may be explained by the fast evaporation of the solvent in electrospinning process may be resulted with more stable PCL structures.

5.2 Contact Angle Measurement of Histidine and Fetuin Modified Poly-ϵ-caprolactone Nanofiber Meshes

Water contact angle values of biomaterial surfaces play a key role to evaluate if a surface suitable for the cells or not. As explained by Ratner et al. and Liang et al. previously, surface wettability has high correlation with the cell adhesion and spreading. As a common agreement hydrophobic surfaces (low surface energy) lead poor cell spreading while hydrophilic surfaces (high surface energy) are leading satisfying cell spreading [75, 76]. In this context, surface wettablity properties of HMDA modified, histidine and fetuin immobilized PCL nanofibers were investigated. PCL generally shows moderate biodegradability and biocompatibility; however, the actual utilization of this material is limited by its hydrophobicity [77, 78]. The incorporation of histidine and fetuin improve the hydrophilicity of PCL/HMDA, PCL/HMDA/His, PCL/HMDA/Fetuin, nanofiber meshes. This might be attributed to the amine and carboxylic and imidazole functional groups of histidine and hydrophilic amino acid side chains of fetuin protein whereas such functional groups are not present in PCL structure [77, 79].

5.3 FT-IR Spectra of Modified Poly-ϵ-caprolactone Nanofiber Meshes

ATR-FTIR was used to investigate the chemical functional groups that were present on the surfaces of the PCL nanofiber meshes after modification with HDMA,

histidine, fetuin. As mentioned at result section. Characteristic carbonyl ester bond of PCL was observed at 1725 cm^{-1} that was very close in wavelength in the literature [67, 68]. After modification with HMDA, the carbonyl ester peak was shift to lower wavenumber, 1721 cm^{-1}. There were no signals due to the N-H stretching of the amino groups but there was a shifted the carbonyl (C=O) stretching of the amide linkage that was observed at 1652 cm^{-1} on (expected 1640 cm^{-1}) the difference spectrum which is an evidence of the reaction of HMDA with PCL. This could be a result of the extremely low concentration of-NH_2 groups available for detection by the instrument (the sampling depth of ATR-FTIR was 1-2 μm) [65].

Characteristic carbonyl ester peak of PCL was also observed at 1725 cm^{-1} before histidine and fetuin immobilization. After histidine and fetuin immobilization carbonyl bonds were shifted to 1726 cm^{-1} and 1733 cm^{-1}, respectively. At 1558 cm^{-1}, histidine's imidazole rings vibrations were observed and that is a confirmation for the histidine modification [80]. In the spectrum of fetuin immobilized PCL nanofiber meshes, two bonds at 1652 cm^{-1} and 1559 cm^{-1} were recorded which correspond to amide I and amide II bands. Normally, 1650 cm^{-1} (amide I) and 1540 cm^{-1} (amide II), correspond to the stretching vibrations of C=O bond, and coupling of bending of N-H bond and stretching of C-N bonds, respectively. The shifts of the amide I and amide II bonds were attributable to the interaction of HMDA and Fetuin[81].

5.4 XPS Results of Poly-ϵ-caprolactone Membranes

The surface chemistry of the PCL plain meshes and the PCL nanfiber membranes for C1s and O1s levels was characterized by using the X-rays Photoelectron Spectroscopy and shown in Figure 4.10a and Figure 4.11a. As can be seen from the figure 4.10e and the figure 4.11e, the high resolution XPS spectra of the C1s for PCL plain membrane and PCL nanofiber meshes was resolved into three different peaks that were found as C-H/C-C, C-O, and O=C-O bonds [40]. Schematic diagram shows the PCL molecule which implies that all specific bonds of the molecule were found (4.12).

Schematic diagram after aminolysis demonstrates the reaction between the ester group (-COO-) of PCL molecule and amine groups (-NH_2) of 1,6-hexanediamine (HMDA) [65, 82]. The XPS survey spectrum and the N1s core level spectrum of HMDA modified the PCL membrane clearly indicates a considerable degree of aminolysis. In the analysis of N1s core level spectra, two new peaks for PCL plain membrane and PCL nanofiber mesh were appeared at 399.32 eV and 399.59 eV for C-NH_2 free amino groups and at 401.24 eV and 400.85 eV for O=C-NH amide groups, respectively (Figure 4.10d , Figure 4.11d) [83, 84], In the analysis of C1s core level spectra of HMDA modified the PCL plain membrane, the high binding energy peak was found at 288.46 eV which is assigned to carboxylate (O=C-OH) and amide carbon (N-C=O) (Figure 4.10f) [82]. The peak at 285.89 eV was found that amine (C-N) and carbonyl (C-O) groups can be characterized in the C1s core level spectra (Figure 4.10f). In the analysis of the C1s core level spectra of HMDA modified the PCL nanofiber mesh, the new peak as amine bonds (C-N) was found at 285.14 eV from HMDA and was shown in Figure 4.11f. The high binding energy peak at 288.54 eV is attributed to carboxylate (O=C-OH) and amide carbon (N-C=O) of HMDA modified the PCL nanofiber mesh (Figure 4.11f) [82]. The XPS survey results of HMDA modified the PCL membranes can be affected from the either the unreaction of amino groups with ester groups or the penetration of molecules into the PCL membrane due to the existence of the deep pores [18, 65].

Chemical modifications of the PCL membrane at different concentrations of His/HMDA ratio were shown in the schematic diagram. The raw data spectra of C1s, N1s and O1s, spectra of 1:1, 1:2, and 1:4 His/HMDA modified the PCL membrane were shown that the unknown penetration ratio of histidine and 1,6-hexanediamine molecules into the PCL membranes were observed because of the deep pores in the PCL membrane [18]. Schematic diagram shows the histidine that has a side-chain containing an imidazole group, resulting in a total of three nitrogen atoms in the molecule [84]. The high-resolution N1s spectra of 1:4, 1:2, and 1:1 His/HMDA modified the PCL membrane were appeared the NH-C=O and C-N bonds. Addition to these bonds, aromatic N was found in the analysis of the N1s spectra of 1:4 His/HMDA modified PCL plain membrane. The peak at 398.08 eV, attributable to N=C-NH, was measured in the analysis of the N1s spectra of 1:1, 1:2 His/HMDA modified PCL plain membrane.

The peak at 400.47 eV coressponding to N=C-NH bond was found in the analysis of the N1s core level spectra of 1:4 His/HMDA modified PCL nanofiber [84, 85].

The X-rays Photoelectron Spectroscopy was studied to investigate the reaction between Fetuin and HMDA modified PCL membrane as shown in Figure 4.21a and the Figure 4.22a. The appearance of a strong N1s level in the XPS survey spectrum of the PCL membrane was contributed from the presence of fetuin. As can be seen from the figure 4.21c, the N1s high-resolution spectrum of the PCL plain membrane shows three different binding energies that were assigned to C-N, O=C-N and C-NH bonds at 399.36 eV, 400.82 eV and 401.66 eV, respectively. Figure 4.22c show that the analysis of N1s core level spectrum of the PCL nanofiber mesh was appeared at 399.48 eV and 401.16 eV the corresponding to C-N and O=C-NH, respectively [84]. The amount of N1s level of the modified PCL plain membrane is more than the amount of N1s level of the modified PCL nanofiber membrane due to deep pores of nanofiber structures. The C1s core level for the PCL membrane can be resolved into five different peaks that are assigned to C-C/C-H, C=C, C-N/C-S/C-O, O=C-N and O=C-O peaks [82].

5.5 Cell Studies

Proliferation of L929 cells on the histidine and fetuin modified PCL membranes and nanofiber meshes at day 2 were determined by using MTT assay [86]. Chemical (HMDA) and biochemical (histidine amino acid and fetuin protein) on cellular behavior were investigated according to the proliferation percent versus control groups. The number of cells on histidine modified PCL membranes and nanofibers were significantly increased compared to control (TCPS) and unmodified PCL membranes and nanofiber meshes with an increasing histidine amino acid content. The effect of histidine immobilization was clearly observed on the cell proliferation. The number of cells were increased to 127.6 $\pm$ 3.3% and 158.7 $\pm$ 5.1% on PCL/HDMA/His (1:1 mole ratio) membranes and nanofiber meshes respectively. This result may be due to the increased hydrophilicity of the modified PCL structures (membrane and nanofiber) because of the modification with hydrophilic histidine amino acid. Histidine amino acid

has a hydropaty index of -3.2 which means a hydrophilic molecule [87]. Histidine is a basic and essential amino acid with a positively charged imidazole ring which also gave a biofunctional property to the modified surfaces. The effect of histidine amount in cell proliferation was also clearly observed on both PCL structures as increasing the ligand density resulted with increased cell proliferation percentages. On both PCL membranes and nanofiber meshes modified with HMDA showed lower cell proliferation percentages than the control and histidine modified groups. HDMA modification increases the hydrophilicity of the surface. However, this modification wasn't provoke the cell proliferation. This might be the inaccessibility of the receptors of fibroblast cells to the surface amino groups of PCL membranes and nanofiber meshes. Histidine amino acid is a bigger molecule that the cells interact much more easily with their receptors. From the cell proliferation data we couldn't observe any positive effect of fetuin immobilization to PCL membranes and nanofibers. This may be due to using low amount of fetuin in immobilization and some of the fetuin molecules immobilized to the inner pores of PCL membranes and underneath the surface of nanofibers with low accessibility. The effect of surface topography was also observed from the cell proliferation data. Histidine modified PCL nanofibers were shown better cell proliferation rate than histidine modified PCL membranes. Over all, modification of PCL membranes and nanofiber with a simple biomolecule, histidine amino acid increased cell proliferation of L929 fibroblast cells. In the literature several groups have worked on modified PCL electrospun nanofibers. Guatam et al modified PCL nanofiber with gelatin which is a more complex structure but, biocompatible, biodegradable, and natural biopolymer derived from collagen and showed lower cell proliferation percent than histidine modified PCL structures [86]. Tığlı et al was investigated the cellular behavior on epidermal growth factor (EGF) immobilized PCL/gelatin nanofibrous scaffolds and obtained similiar results [77]. Dubas et al were studied the coating of polyelectrolyte multilayer thin films on nanofibrous scaffolds to improve cell adhesion and observed a close improvement like in our study [88].

5.6 Future Work

In this thesis, histidine and fetuin were immobilized onto Poly-ϵ-caprolactone (PCL) membranes and nanofiber meshes prepared and L929 cells proliferation was investigated on these scaffolds. A simple amino acid (histidine) on the surface has caused noticeable enhancement of proliferation of cells. The results are promising that these surfaces may be used in many different tissue engineering applications. However, more experiments are needed to be done to understand cellular behaviour such as adhesion, viability on these surfaces.

REFERENCES

1. Heath, C. A., and G. E. Rutkowski, "The development of bioartificial nerve grafts for peripheral-nerve regeneration," *Tibtech*, Vol. 16, pp. 163–168, April 1998.

2. Zhong, Y., and R. V. Bellamkondai, "Biomaterials for the central nervous system," *Journal of The Roya Society Interfacel*, Vol. 5, pp. 957–975, May 2008.

3. Yao, L., S. Wang, W. Cui, R. Sherlock, C. O'Connel, G. Damodaran, A. Gorman, A. Windebank, and A. Panditi, "Effect of functionalized micropatterned plga on guided neurite growth," *Acta Biomaterialia*, pp. 580–588, September 2008.

4. Patel, S., K. Kurpinski, R. Quigley, H. Gao, B. S. Hsiao, M.-M. Poo, and S. Li, "Bioactive nanofibers: Synergistic effects of nanotopography and chemical signaling on cell guidance," *Nano Letters*, Vol. 7, pp. 2122–2128, June 2007.

5. Selim, M., A. J. Bullock, K. A. Blackwood, C. R. Chapple, and S. MacNeil, "Developing biodegradable scaffolds for tissue engineering of the urethra," *BJU International*, Vol. 107, pp. 296–302, January 2010.

6. Hossain, S. M. Z., S. M. E. Babar, S. G. Azam, S. N. Sarma, and G. D. Haki, "Spinal cord injury treatment using a noble biocompatible bridge," *Molecular & Cellular Toxicology*, Vol. 3, pp. 151–158, September 2007.

7. Gwon, A., and L. Gruber, "Engineering the crystalline lens with a biodegradable or non-degradable scaffold," *Experimental Eye Research*, Vol. 91, pp. 220–228, August 2010.

8. Horst, O. V., M. G. Chavez, A. H. Jheon, T. Desai, and O. D. Klein, "Stem cell and biomaterials research in dental tissue engineering and regeneration," *Dental Clinics of North America*, Vol. 56, pp. 495–520, July 2012.

9. Pavia, F. C., S. Rigogliuso, V. L. Carrubba, G. A. Mannella, G. Ghersi, and V. Brucato, "Poly lactic acid based scaffolds for vascular tissue engineering," *Chemical Engineering Transactions*, Vol. 27, pp. 409–414, June 2012.

10. Domingos, M., D. Dinucci, S. Cometa, M. Alderighi, P. J. Bartolo, and F. Chiellini, "Polycaprolactone scaffolds fabricated via bioextrusion for tissue engineering applications," *International Journal of Biomaterials*, Vol. 2009, June 2009.

11. Baumchen, F., R. Smeets, D. Koch, and H. G. Graber, "The impact of defined polyglycolide scaffold structure on the proliferation of gingival fibroblasts in vitro: a pilot study," *Oral and maxillofacial surgery*, Vol. 108, pp. 505–513, October 2009.

12. Woodruff, M. A., and D. W. Hutmacherl, "The return of a forgotten polymer-polycaprolactone in the 21 st century," *Progress in Polymer Science*, Vol. 35, pp. 1–40, April 2010.

13. Pettikiriarachchi, J. T. S., C. L. Parish, M. S. Shoichet, J. S. Forsythe, and D. R. Nisbet, "Biomaterials for brain tissue engineering," *Australian Journal of Chemistry*, pp. 1143–1154, June 2010.

14. Lam, C. X. F., M. M. Savalani, S.-H. Teoh, and D. W. Hutmacher, "Dynamics of in vitro polymer degradation of polycaprolactone-based scaffolds: accelerated versus simulated physiological conditions," *Biomedical Materials*, Vol. 3, pp. 1–15, August 2008. Available at: stacks.iop.org/BMM/3/034108.

15. Sinha, V., K. Bansal, R. Kaushik, R. Kumria, and A. Trehan, "Poly-caprolactone microspheres and nanospheres an overview," *International Journal of Pharmaceutics*, Vol. 278, pp. 1–23, April 2004.

16. Shin, M., O. Ishii, T. Sueda, and J. Vacanti, "Contractile cardiac grafts using a novel nanofibrous mesh," *International Journal Biopharma Research*, Vol. 25, pp. 3717–3723, October 2003.

17. Ishii, O., M. Shin, T. Sueda, and J. P. Vacanti, "In vitro tissue engineering of a cardiac graft using a degradable scaffold with an extracellular matrix-like topography," *The Journal of Thoracic and Cardiovascular Surgery*, Vol. 130, pp. 1358–1363, November 2005.

18. Zhu, Y., C. Gao, X. Liu, and J. Shen, "Surface modification of polycaprolactone membrane via aminolysis and biomacromolecule immobilization for promoting cytocompatibility of human endothelial cells," *Biomacromolecules*, Vol. 3, pp. 1312–1319, September 2002.

19. R.Sravanthi, "Preparation and characterization of polycaprolactone pcl scaffolds for tissue engineering application," Master's thesis, National Institute of Technology Rourkela, ORISSA, 2009.

20. Chang, H., and P. D. E. Yiwei Wang, *Cell Responses to Surface and Architecture of Tissue Engineering Scaffolds, Regenerative Medicine and Tissue Engineering - Cells and Biomaterials*, pp. 569–589. China: InTech, August 2011. Available at: http://www.intechopen.com/books/regenerative-medicineand-tissue-engineering-cells-and-biomaterials.

21. Guertin, D. A., and D. M. Sabatini, "Cell size control," *Encyclopedia of Life Sciences*, Vol. 22, pp. 1–10, January 2006.

22. Zhang, S., F. Gelain, and X. Zhao, "Designer self-assembling peptide nanofiber scaffolds for 3d tissue cell cultures," *Seminars in Cancer Biology*, Vol. 15, pp. 413–420, October 2005.

23. Schindler, M., I. Ahmed, J. Kamal, A. Nur-E-Kamal, T. H. Grafe, H. Y. Chung, and S. Meiners, "A synthetic nanofibrillar matrix promotes in vivo-like organization and morphogenesis for cells in culture," *Biomaterials*, Vol. 26, pp. 5624–5631, February 2005.

24. Woo, K. M., J.-H. Jun, V. J. Chen, J. Seo, J.-H. Baek, H.-M. Ryoo, G.-S. Kim, M. J. Somerman, and P. X. Ma, "Nano-fibrous scaffolding promotes osteoblast differentiation and biomineralization," *Biomaterials*, Vol. 28, pp. 335–343, June 2006.

25. Woo, K. M., V. J. Chen, and P. X. Ma, "Nano-fibrous scaffolding architecture selectively enhances protein adsorption contributing to cell attachment," *Journal of BiomedMaterial Research Part A*, Vol. 67A, pp. 531–537, March 2003.

26. Xu, C., R. Inai, M. Kotaki, and S. Ramakrishna, "Aligned biodegradable nanofibrous structure: a potential scaffold for blood vessel engineering," *Biomaterials*, Vol. 25, pp. 877–886, February 2004.

27. Yang, F., C. Y. Xu, M. Kotaki, S. Wang, and S. Ramakrishna, "Characterization of neural stem cells on electrospun poly(l-lactic acid) nanofibrous scaffold," *Journal of Biomaterials Science*, Vol. 15, pp. 1483–1497, April 2004.

28. e Kamal, A. N., I. Ahmed, J. Kamal, M. Scindler, and S. Meiners, "Three-dimensional nanofibrillar surfaces promote self-renewal in mouse embryonic stem cells," *Stem Cells*, Vol. 24, pp. 426–433, February 2006.

29. Vasita, R., and D. S. Katti, "Nanofibers and their applications in tissue engineering," *International Journal of Nanomedicine*, Vol. 1, pp. 15–30, April 2006.

30. Henstock, D. J. R., *Porous Silicon Polycaprolactone Composites for Orthopaedic Tissue Engineering.* PhD thesis, School of Biomedical Sciences Medical School University of Nottingham, Nottingham, UK, 2009.

31. Patel, N. R., and P. P. Gohil, "A review on biomaterials: Scope, applications & human anatomy significance," *International Journal of Emerging Technology and Advanced Engineering*, Vol. 2, pp. 92–101, April 2012.

32. Patel, P. N., K. G. Parmar, A. N. Nakum, M. N. Patel, P. R. Patel, V. R. Patel, and D. D. J. Sen, "Biodegradable polymers: An ecofriendly approach in newer millenium.," *Asian Journal of Biomedical and Pharmaceutical Sciences*, Vol. 1, pp. 23–39, July 2011.

33. Naira, L. S., and C. T. Laurencinl, "Biodegradable polymers as biomaterials," *Progress in Polymer Sciencel*, Vol. 2007, pp. 762–798, June 2007.

34. Hsu, C.-M., *Electrospinning of Poly(Caprolactone).* PhD thesis, Worcester Polytechnic Institute, 2003.

35. Hoglund, A., "Controllable degradation product migration from biomedical polyesterethers," Master's thesis, KTH Chemical Sciences and Engineering, Stocholm, Sweden, 2007.

36. Bezwada, R. S., D. D. Jamiolkowski, I.-Y. Lee, V. Agarwal, J. Persivale, S. Trenka-Benthin, M. Erneta, J. Suryadevara, A. Yang, and S. Liu, "Monocryl suture, a new ultrapliable absorbable monofilament suture," *Biomaterials*, Vol. 16, pp. 1141–1148, October 1995.

37. Moes-Carpi, M. M., and S. Sherwood, "Polycaprolactone for the correction of nasolabial folds: A 24-month, prospective, randomized, controlled clinical trial," *the American Society for Dermatologic Surgery*, Vol. 39, pp. 457–463, January 2013.

38. Zopf, D. A., S. J. Hollister, M. E. Nelson, R. G. Ohye, and G. E. Green, "Bioresorbable airway splint created with a three-dimensional printer," *The New England Journal of Medicine*, Vol. 21, pp. 2043–2045, May 2013.

39. Low, S., Y. N, T. Yeo, and N. Chou, "Use of osteoplug polycaprolactone implants as novel burr-hole covers," *Singapore Medical*, Vol. 8, pp. 777–780, August 2009.

40. Yuan, S., G. Xiong, A. Roguin, S. H. Teoh, and C. Choong, "Amelioration of blood compatibility and endothelialization of polycaprolactone substrates by surface-initiated atom transfer radical polymerization," *Advances in Biomaterials Science and Biomedical Applications*, pp. 177–205, 2013. Available at: http://dx.doi.org/10.5772/52646.

41. Varela, M. C., M. Guzman, J. Molpeceres, M. del Rosario Aberturas, D. Rodriguez-Puyol, and M. Rodriguez-Puyol, "Cyclosporine-loaded polycaprolactone nanoparticles: immunosuppression and nephrotoxicity in rats," *European Journal of Pharmaceutical Sciences*, pp. 471–478, December 2001.

42. Liu, L., S. Guo, J. Chang, C. Ning, C. Dong, and D. Yanl, "Surface modification of polycaprolactone membrane via layer-by-layer deposition for promoting blood compatibility," *Journal of Biomedical Materials Research Part B: Applied Biomaterials*, pp. 244–250, April 2008.

43. woon Choi, H., J. K. Johnson, J. Nam, D. F. Farson, and J. Lannutti, "Structuring electrospun polycaprolactone nanofiber tissue scaffolds by femtosecond laser ablation," *Journal of Lazer Applications*, Vol. 19, pp. 244–250, November 2007.

44. Gibson, P. W., C. Lee, F. Ko, and D. Reneker, "Application of nanofiber technology to nonwoven thermal insulation," *Journal of Engineered Fibers and Fabrics*, Vol. 2, no. 2, pp. 32–40, 2007.

45. Smith, I. O., X. H. Liu, L. A. Smith, and P. X. Ma, "Nanostructured polymer scaffolds for tissue engineering and regenerative medicine.," *WIREs Nanomedicine and Nanobiotechnologyl*, Vol. 1, pp. 226–236, April 2009.

46. Bajakova, J., J. Chaloupek, D. Lukas, and M. Lacain, "Drawing- the production of individual nanofibers by experimental method," *Nanocon2011*, September 2011.

47. Padron, S., A. Fuentes, D. Caruntu, and K. Lozano, "Experimental study of nanofiber production through forcespinning," *Journal Of Applied Physics*, Vol. 113, January 2013. Available at: http://dx.doi.org/10.1063/1.4769886.

48. Ellison, C. J., A. Phatak, D. W. Giles, C. W. Macosko, and F. S. Bates, "Melt blown nanofibers: Fiber diameter distributions and onset of fiber breakup," *Polymer*, Vol. 48, pp. 3306–3316, April 2007.

49. Pokorny, P., L. Kocis, J. Chvojka, D. Lukas, J. Beran, M. Bilek, and K. Pejchar, "Alternating current electrospinning method for preparation of nanofibrous materials," *Nanocon2013*, October 2013.

50. Temenoff, J. S., and A. G. Mikos, *Biomaterials The Intersection of Biology and Material Science*, New Jersay: Pearson Pretice Hall, 2008.

51. Rim, N. G., C. S. Shin, and H. Shin, "Current approaches to electrospun nanofibers for tissue engineering," *Biomedical Materials*, Vol. 8, January 2013.

52. Bhardwaj, N., and S. C. Kundua, "Electrospinning: A fascinating fiber fabrication technique," *Biotechnology Advances*, pp. 325–347, January 2010.

53. Haghi, A. K., and M. Akbari, "Trends in electrospinning of natural nanofibers," *physica status solidi*, Vol. 204, pp. 1830–1834, May 2007.

54. Priyakumar, U. D., M. Punnagai, G. P. K. Mohan, and G. N. Sastry, "A computational study of cation-p interactions in polycyclic systems: exploring the dependence on the curvature and electronic factors," *Tetrahedron*, Vol. 60, pp. 3037–3043, March 2004.

55. Uchida, K., "Histidine and lysine as targets of oxidative modification," *Amino Acids*, Vol. 25, pp. 249–257, July 2003.

56. Remko, M., D. Fitz, and B. M. Rode, "Effect of metal ions (li+, na+, k+, mg2+, ca2+, ni2+, cu2+ and zn2+) and water coordination on the structure and properties of l-histidine and zwitterionic l-histidine," *Amino Acids*, Vol. 39, pp. 1309–1319, November 2010.

57. Li, F., D. Fitz, D. G. Fraser, and B. M. Rode, "Catalytic effects of histidine enantiomers and glycine on the formation of dileucine and dimethionine in the salt-induced peptide formation reaction," *Amino Acids*, Vol. 38, pp. 287–294, January 2010.

58. Mathews, C. K., and K. E. van Holde, *Biochemistry*, pp. 137–140. The Benjamin Cummings, 1990.

59. Vijayalakshmi, M. A., "Histidine ligand affinity chromatography," *Molecular Biotechnology*, Vol. 6, pp. 347–357, December 1996. Available at: stacks.iop.org/BMM/3/034108.

60. Vani, P., M. Swarna, N. Uma, M. Kinnera, N. Prasad, and I. S. Babui, "A protective role of fetuin-a, in heart failure and diabetes activities," *International Journal Biopharma Research*, Vol. 21, pp. 112–116, February 2013.

61. Kitchener, P. D., K. M. Dziegielewska, E. J. Hutton, C. F. L. Hinrichsen, and N. R. Saundersi, "Fetuin in neurons of the retina and cerebellum during fetal and postnatal development of the rat," *International Journal Development Neuroscience*, Vol. 17, pp. 21–30, February 1999.

62. Hausler, M., C. Schafer, C. Osterwinter, and W. Jahnen-Dechent, "The physiologic development of fetuin-a serum concentrations in children," *International Journal Biopharma Research*, Vol. 66, pp. 660–664, August 2009.

63. Ochieng, J., and G. Chaudhuri, "Cystatin superfamily," *Journal of Health Care for the Poor and Underserved*, Vol. 21, pp. 51–70, February 2010.

64. Zargarian, S. S., and V. Haddadi-Asl, "A nanofibrous composite scaffold of pcl/hydroxyapatite-chitosan/pva prepared by electrospinning.," *Iranian Polymer Journal*, Vol. 19, pp. 457–468, April 2010.

65. Mattanavee, W., O. Suwantong, S. Puthong, T. Bunaprasert, V. P. Hoven, and P. Supaphol, "Immobilization of biomolecules on the surface of electrospun polycaprolactone fibrous scaffolds for tissue engineering," *Applied Material and Interfaces*, Vol. 1, pp. 1076–1085, May 2009.

66. Garipcan, B., S. Odabas, G. Demirel, J. Burger, S. S. Nonnenmann, M. T. Coster, E. M. Gallo, B. Nabet, J. E. Spanier, and E. Piskin, "In vitro biocompatibility of n-type and undoped silicon nanowires," *Advanced Engineering Materials*, Vol. 13, pp. B3–B9, February 2011.

67. Elzubair, A., C. N. Elias, J. C. M. Suarez, H. P. Lopes, and M. V. B. Vieira, "The physical characterization of a thermoplastic polymer for endodontic obturation," *Journal of Dentistry*, Vol. 34, pp. 784–789, November 2006.

68. Elzein, T., M. Nasser-Eddine, C. Delaite, S. Bistac, and P. Dumas, "Ftir study of polycaprolactone chain organization at interfaces," *Journal of Colloid and Interface Science*, Vol. 273, pp. 381–387, May 2004.

69. "Fetuin product information," tech. rep., Sigma Aldrich, USA, December 2013. Available at: http://www.sigmaaldrich.com.

70. Zhou, F.-L., and R.-H. Gong, "Manufacturing technologies of polymeric nanofibres and nanofibre yarns," *Polymer International*, Vol. 57, pp. 837–845, June 2008.

71. Xie, Z., *Biomedical Materials Based on Electrospun Polymeric Fibers*. PhD thesis, Auburn University, Alabama, 2010.

72. Podgorski, A., A. Balazy, and L. Gradon, "Application of nanofibers to improve the filtration efficiency of the most penetrating aerosol particles in fibrous filters," *Chemical Engineering Science*, Vol. 61, pp. 6804–6815, July 2006.

73. Haghi, A. K., *Electrospinning of Nanofibers in Textiles.* Canada: CRC Press, 2012.

74. Tang, Z., R. Black, J. Curran, J. Hunt, N. Rhodes, and D. Williams, "Surface properties and biocompatibility of solvent-cast poly[caprolactone] films," *Biomaterials*, Vol. 25, pp. 4741–4748, August 2004.

75. Hao, L., and J. Lawrence, *Laser Surface Treatment of Bio-Implant Materials.* England: John Wiley & Sons Ltd, October 2005.

76. Ratner, B. D., A. S. Hoffman, F. J. Schoen, and J. E. Lemons, *Biomaterials science An Introduction to Materials in Medicine.* California: Academic Press, 1996.

77. Tigli, R. S., N. M. Kazaroglu, B. Mavis, and M. Gumusderelioglu, "Cellular behavior on epidermal growth factor (egf)-immobilized pclgelatin nanofibrous scaffolds," *Journal of Biomaterials Science*, Vol. 22, pp. 207–223, Jun 2011.

78. Zhu, Y., C. Gao, and J. Shen, "Surface modification of polycaprolactone with poly(methacrylic acid) and gelatin covalent immobilization for promoting its cytocompatibility," *Biomaterials*, pp. 4889–4895, February 2012.

79. Ghasemi-Mobarakeh, L., M. P. Prabhakaran, M. Morshed, M.-H. Nasr-Esfahani, and S. Ramakrishna, "Electrospun poly(caprolactone)/gelatin nanofibrous scaffolds for nerve tissue engineering," *Biomaterials*, Vol. 25, pp. 4532–4539, December 2008.

80. Banerjee, S., T. K. Paira, A. Kotal, and T. K. Mandal, "Surface-confined atom transfer radical polymerization from sacrificial mesoporous silica nanospheres for preparing mesoporous polymer/carbon nanospheres with faithful shape replication: Functional mesoporous materials," *Advanced Functional Materials*, Vol. 22, pp. 4751–4762, November 2012.

81. Hua, X., S.-H. Parka, E. S. Gila, X.-X. Xiaa, A. S. Weissb, and D. L. Kaplan, "The influence of elasticity and surface roughness on myogenic and osteogenic-differentiation of cells on silk-elastin biomaterials," *Biomaterials*, Vol. 32, pp. 8979–8989, December 2011.

82. Bratt, A., and A. R. Barron, "Xps of carbon nanomaterials," *OpenStax-CNX*, Vol. module: m34549, February 2011. Available at: http://cnx.org/content/m34549/1.2/.

83. Yang, Z., M. ZhengWei, S. HuaYu, and G. ChangYou, "In-depth study on aminolysis of poly(caprolactone): Back to the fundamentals," *Science China Chemistry*, Vol. 55, pp. 2419–2427, November 2012.

84. Stevens, J. S., A. C. de Luca, M. Pelendritis, G. Terenghi, S. Downes, and S. L. M. Schroeder, "Quantitative analysis of complex amino acids and rgd peptides by x-ray photoelectron spectroscopy (xps)," *Surface and Interface Analysis*, Vol. 45, pp. 1238–1246, August 2013.

85. Beamson, G., and D. Briggs, *High Resolution XPS of Organic Polymers - The Scienta ESCA300 Database*, p. 140. Chichester: Wiley, 1992.

86. Gautam, S., A. K. Dinda, and N. C. Mishra, "Fabrication and characterization of pcl/gelatin composite nanofibrous scaffold for tissue engineering applications by electrospinning method," *Materials Science and Engineering: C*, Vol. 33, pp. 1228–1235, April 2013.

87. Kyte, J., and R. F. Doolittle, "A simple method for displaying the hydropathic character of a protein," *Journal of Molecular Biology*, Vol. 157, pp. 105–132, May 1982.

88. Dubas, S. T., P. Kittitheeranun, R. Rangkupan, N. Sanchavanakit, and P. Potiyaraj, "Coating of polyelectrolyte multilayer thin films on nanofibrous scaffolds to improve cell adhesion," *Journal of Applied Polymer Science*, Vol. 114, pp. 1574–1579, November 2009.

89. Lamport, L., *A Document Preparation System LateX*, New York: Addison–Wesley, 2nd ed., 1994.